The transmembrane domain of hepatitis C virus E1 glycoprotein induces cell death. *Virus Res* **104**, 1–9.

D'Agostino, D. M., Ranzato, L., Arrigoni, G. & 10 other authors (2002). Mitochondrial alterations induced by the p13^{II} protein of human T-cell leukemia virus type 1. *J Biol Chem* 277, 34424–34433.

Davis, S., Weiss, M. J., Wong, J. R., Lampidis, T. J. & Chen, L. B. (1985). Mitochondrial and plasma membrane potentials cause unusual accumulation and retention of rhodamine 123 by human breast adenocarcinoma-derived MCF-7 cells. *J Biol Chem* **260**, 13844–13850.

Deng, L., Nagano-Fujii, M., Tanaka, M., Nomura-Takigawa, Y., Ikeda, M., Kato, N., Sada, K. & Hotta, H. (2006). NS3 protein of *Hepatitis C virus* associates with the tumour suppressor p53 and inhibits its function in an NS3 sequence-dependent manner. *J Gen Virol* **87**, 1703–1713.

Deveraux, Q. L., Roy, N., Stennicke, H. R., Van Arsdale, T., Zhou, Q., Srinivasula, S. M., Alnemri, E. S., Salvesen, G. S. & Reed, J. C. (1998). IAPs block apoptotic events induced by caspase-8 and cytochrome *c* by direct inhibition of distinct caspases. *EMBO J* **17**, 2215–2223.

Egger, D., Wölk, B., Gosert, R., Bianchi, L., Blum, H. E., Moradpour, D. & Bienz, K. (2002). Expression of hepatitis C virus proteins induces distinct membrane alterations including a candidate viral replication complex. *J Virol* **76**, 5974–5984.

Eguchi, Y., Shimizu, S. & Tsujimoto, Y. (1997). Intracellular ATP levels determine cell death fate by apoptosis or necrosis. *Cancer Res* **57**, 1835–1840.

Erdtmann, L., Franck, N., Lerat, H., Seyec, J. L., Gilot, D., Cannie, I., Gripon, P., Hibner, U. & Guguen-Guillouzo, C. (2003). The hepatitis C virus NS2 protein is an inhibitor of CIDE-B-induced apoptosis. *J Biol Chem* **278**, 18256–18264.

Everett, H., Barry, M., Sun, X., Lee, S. F., Frantz, C., Berthiaume, L. G., McFadden, G. & Bleackley, R. C. (2002). The myxoma poxvirus protein, M11L, prevents apoptosis by direct interaction with the mitochondrial permeability transition pore. *J Exp Med* **196**, 1127–1139.

Failla, C., Tomei, L. & De Francesco, R. (1995). An amino-terminal domain of the hepatitis C virus NS3 protease is essential for interaction with NS4A. *J Virol* **69**, 1769–1777.

Fearnhead, H. O., Rodriguez, J., Govek, E.-E., Guo, W., Kobayashi, R., Hannon, G. & Lazebnik, Y. A. (1998). Oncogene-dependent apoptosis is mediated by caspase-9. *Proc Natl Acad Sci U S A* **95**, 13664–13669.

Feng, P., Park, J., Lee, B.-S., Lee, S.-H., Bram, R. J. & Jung, J. U. (2002). Kaposi's sarcoma-associated herpesvirus mitochondrial K7 protein targets a cellular calcium-modulating cyclophilin ligand to modulate intracellular calcium concentration and inhibit apoptosis. *J Virol* **76**, 11491–11504.

Florese, R. H., Nagano-Fujii, M., Iwanaga, Y., Hidajat, R. & Hotta, H. (2002). Inhibition of protein synthesis by the nonstructural proteins NS4A and NS4B of hepatitis C virus. *Virus Res* **90**, 119–131.

Fujita, T., Ishido, S., Muramatsu, S., Itoh, M. & Hotta, H. (1996). Suppression of actinomycin D-induced apoptosis by the NS3 protein of hepatitis C virus. *Biochem Biophys Res Commun* **229**, 825–831.

Gewies, A., Rokhlin, O. W. & Cohen, M. B. (2000). Cytochrome *c* is involved in Fas-mediated apoptosis of prostatic carcinoma cell lines. *Cancer Res* **60**, 2163–2168.

Goldmacher, V. S., Bartle, L. M., Skaletskaya, A. & 10 other authors (1999). A cytomegalovirus-encoded mitochondria-localized inhibitor of apoptosis structurally unrelated to Bcl-2. *Proc Natl Acad Sci U S A* **96**, 12536–12541.

Gosert, R., Egger, D., Lohmann, V., Bartenschlager, R., Blum, H. E., Bienz, K. & Moradpour, D. (2003). Identification of the hepatitis C virus RNA replication complex in Huh-7 cells harboring subgenomic replicons. *J Virol* **77**, 5487–5492.

Gross, A., McDonnell, J. M. & Korsmeyer, S. J. (1999). BCL-2 family members and the mitochondria in apoptosis. *Genes Dev* **13**, 1899–1911.

Hahn, C. S., Cho, Y. G., Kang, B.-S., Lester, I. M. & Hahn, Y. S. (2000). The HCV core protein acts as a positive regulator of Fas-mediated apoptosis in a human lymphoblastoid T cell line. *Virology* **276**, 127–137.

Hayashi, J., Kishihara, Y., Yamaji, K., Furusyo, N., Yamamoto, T., Pae, Y., Etoh, Y., Ikematsu, H. & Kashiwagi, S. (1997). Hepatitis C viral quasispecies and liver damage in patients with chronic hepatitis C virus infection. *Hepatology* **25**, 697–701.

He, Y., Nakao, H., Tan, S.-L., Polyak, S. J., Neddermann, P., Vijaysri, S., Jacobs, B. L. & Katze, M. G. (2002). Subversion of cell signaling pathways by hepatitis C virus nonstructural 5A protein via interaction with Grb2 and P85 phosphatidylinositol 3-kinase. *J Virol* **76**, 9207–9217.

Hidajat, R., Nagano-Fujii, M., Deng, L., Tanaka, M., Takigawa, Y., Kitazawa, S. & Hotta, H. (2005). Hepatitis C virus NS3 protein interacts with ELKS-δ and ELKS-α, members of a novel protein family involved in intracellular transport and secretory pathways. *J Gen Virol* **86**, 2197–2208.

Hiramatsu, N., Hayashi, N., Katayama, K., Mochizuki, K., Kawanishi, Y., Kasahara, A., Fusamoto, H. & Kamada, T. (1994). Immunohistochemical detection of Fas antigen in liver tissue of patients with chronic hepatitis C. *Hepatology* **19**, 1354–1359.

Hsu, E. C., Hsi, B., Hirota-Tsuchihara, M. & 8 other authors (2003). Modified apoptotic molecule (BID) reduces hepatitis C virus infection in mice with chimeric human livers. *Nat Biotechnol* **21**, 519–525.

Ishido, S., Fujita, T. & Hotta, H. (2000). Possible involvement of the NS3 protein of hepatitis C virus in hepatocarcinogenesis: its interaction with the p53 tumor suppressor. In *Hepatocellular Carcinoma: Methods and Protocols*, pp. 37–55. Edited by N. A. Habib. Totowa: Humana Press.

Jacotot, E., Ravagnan, L., Loeffler, M. & 15 other authors (2000). The HIV-1 viral protein R induces apoptosis via a direct effect on the mitochondrial permeability transition pore. *J Exp Med* **191**, 33–45.

Jacotot, E., Ferri, K. F., El Hamel, C. & 17 other authors (2001). Control of mitochondrial membrane permeabilization by adenine nucleotide translocator interacting with HIV-1 viral protein R and Bcl-2. *J Exp Med* **193**, 509–520.

Kato, J., Kato, N., Yoshida, H., Ono-Nita, S. K., Shiratori, Y. & Omata, M. (2002). Hepatitis C virus NS4A and NS4B proteins suppress translation in vivo. *J Med Virol* **66**, 187–199.

Kim, J.-E., Song, W. K., Chung, K. M., Back, S. H. & Jang, S. K. (1999). Subcellular localization of hepatitis C viral proteins in mammalian cells. *Arch Virol* **144**, 329–343.

Kiyosawa, K., Sodeyama, T., Tanaka, E. & 8 other authors (1990). Interrelationship of blood transfusion, non-A, non-B hepatitis and hepatocellular carcinoma: analysis by detection of antibody to hepatitis C virus. *Hepatology* **12**, 671–675.

Kuang, W.-F., Lin, Y.-C., Jean, F., Huang, Y.-W., Tai, C.-L., Chen, D.-S., Chen, P.-J. & Hwang, L.-H. (2004). Hepatitis C virus NS3 RNA helicase activity is modulated by the two domains of NS3 and NS4A. *Biochem Biophys Res Commun* **317**, 211–217.

Lan, K.-H., Sheu, M.-L., Hwang, S.-J. & 8 other authors (2002). HCV NS5A interacts with p53 and inhibits p53-mediated apoptosis. *Oncogene* **21**, 4801–4811.

Leprat, P., Ratinaud, M. H., Maftah, A., Petit, J. M. & Julien, R. (1990). Use of nonyl acridine orange and rhodamine 123 to follow biosynthesis and functional assembly of mitochondrial membrane during L1210 cell cycle. *Exp Cell Res* **186**, 130–137.

Li, L., Lorenzo, P. S., Bogi, K., Blumberg, P. M. & Yuspa, S. H. (1999). Protein kinase Cδ targets mitochondria, alters mitochondrial membrane potential, and induces apoptosis in normal and neoplastic keratinocytes when overexpressed by an adenoviral vector. *Mol Cell Biol* **19**, 8547–8558.

Li, X.-D., Sun, L., Seth, R. B., Pineda, G. & Chen, Z. J. (2005). Hepatitis C virus protease NS3/4A cleaves mitochondrial antiviral signaling protein off the mitochondria to evade innate immunity. *Proc Natl Acad Sci U S A* **102**, 17717–17722.

Lin, C.-F., Chen, C.-L., Chang, W.-T., Jan, M.-S., Hsu, L.-J., Wu, R.-H., Tang, M.-J., Chang, W.-C. & Lin, Y.-S. (2004). Sequential caspase-2 and caspase-8 activation upstream of mitochondria during ceramide- and etoposide-induced apoptosis. *J Biol Chem* **279**, 40755–40761.

Liu, X., Kim, C. N., Yang, J., Jemmerson, R. & Wang, X. (1996). Induction of apoptotic program in cell-free extracts: requirement for dATP and cytochrome c. *Cell* **86**, 147–157.

Lohmann, V., Körner, F., Dobierzewska, A. & Bartenschlager, R. (2001). Mutations in hepatitis C virus RNAs conferring cell culture adaptation. *J Virol* **75**, 1437–1449.

Moorman, J. P., Prayther, D., McVay, D., Hahn, Y. S. & Hahn, C. S. (2003). The C-terminal region of hepatitis C core protein is required for Fas-ligand independent apoptosis in Jurkat cells by facilitating Fas oligomerization. *Virology* **312**, 320–329.

Mottola, G., Cardinali, G., Ceccacci, A., Trozzi, C., Bartholomew, L., Torrisi, M. R., Pedrazzini, E., Bonatti, S. & Migliaccio, G. (2002). Hepatitis C virus nonstructural proteins are localized in a modified endoplasmic reticulum of cells expressing viral subgenomic replicons. *Virology* **293**, 31–43.

Muramatsu, S., Ishido, S., Fujita, T., Itoh, M. & Hotta, H. (1997). Nuclear localization of the NS3 protein of hepatitis C virus and factors affecting the localization. *J Virol* **71**, 4954–4961.

Muzio, M., Chinnaiyan, A. M., Kischkel, F. C. & 11 other authors (1996). FLICE, a novel FADD-homologous ICE/CED-3-like protease, is recruited to the CD95 (Fas/APO-1) death-inducing signaling complex. *Cell* **85**, 817–827.

Pang, P. S., Jankowsky, E., Planet, P. J. & Pyle, A. M. (2002). The hepatitis C viral NS3 protein is a processive DNA helicase with cofactor enhanced RNA unwinding. *EMBO J* **21**, 1168–1176.

Rahmani, Z., Huh, K.-W., Lasher, R. & Siddiqui, A. (2000). Hepatitis B virus X protein colocalizes to mitochondria with a human voltage-dependent anion channel, HVDAC3, and alters its transmembrane potential. *J Virol* **74**, 2840–2846.

Reed, K. E. & Rice, C. M. (2000). Overview of hepatitis C virus genome structure, polyprotein processing, and protein properties. *Curr Top Microbiol Immunol* **242**, 55–84.

Ruggieri, A., Harada, T., Matsuura, Y. & Miyamura, T. (1997). Sensitization to Fas-mediated apoptosis by hepatitis C virus core protein. *Virology* **229**, 68–76.

Ruggieri, A., Murdolo, M. & Rapicetta, M. (2003). Induction of FAS ligand expression in a human hepatoblastoma cell line by HCV core protein. *Virus Res* **97**, 103–110.

Sacco, R., Tsutsumi, T., Suzuki, R. & 8 other authors (2003). Antiapoptotic regulation by hepatitis C virus core protein through up-regulation of inhibitor of caspase-activated DNase. *Virology* **317**, 24–35.

Satoh, S., Tanji, Y., Hijikata, M., Kimura, K. & Shimotohno, K. (1995). The N-terminal region of hepatitis C virus nonstructural protein 3 (NS3) is essential for stable complex formation with NS4A. *J Virol* **69**, 4255–4260.

Schwer, B., Ren, S., Pietschmann, T., Kartenbeck, J., Kaehlcke, K., Bartenschlager, R., Yen, T. S. B. & Ott, M. (2004). Targeting of hepatitis C virus core protein to mitochondria through a novel C-terminal localization motif. *J Virol* **78**, 7958–7968.

Shu, H.-B., Halpin, D. R. & Goeddel, D. V. (1997). Casper is a FADD- and caspase-related inducer of apoptosis. *Immunity* **6**, 751–763.

Siavoshian, S., Abraham, J. D., Thumann, C., Kieny, M. P. & Schuster, C. (2005). Hepatitis C virus core, NS3, NS5A, NS5B proteins induce apoptosis in mature dendritic cells. *J Med Virol* **75**, 402–411.

Skulachev, V. P. (1998). Cytochrome *c* in the apoptotic and antioxidant cascades. *FEBS Lett* **423**, 275–280.

Soguero, C., Joo, M., Chianese-Bullock, K. A., Nguyen, D. T., Tung, K. & Hahn, Y. S. (2002). Hepatitis C virus core protein leads to immune suppression and liver damage in a transgenic murine model. *J Virol* **76**, 9345–9354.

Song, J., Fujii, M., Wang, F., Itoh, M. & Hotta, H. (1999). The NS5A protein of hepatitis C virus partially inhibits the antiviral activity of interferon. *J Gen Virol* **80**, 879–886.

Sung, V. M.-H., Shimodaira, S., Doughty, A. L., Picchio, G. R., Can, H., Yen, T. S. B., Lindsay, K. L., Levine, A. M. & Lai, M. M. C. (2003). Establishment of B-cell lymphoma cell lines persistently infected with hepatitis C virus in vivo and in vitro: the apoptotic effects of virus infection. *J Virol* **77**, 2134–2146.

Taguchi, T., Nagano-Fujii, M., Akutsu, M., Kadoya, H., Ohgimoto, S., Ishido, S. & Hotta, H. (2004). Hepatitis C virus NS5A protein interacts with 2′,5′-oligoadenylate synthetase and inhibits antiviral activity of IFN in an IFN sensitivity-determining region-independent manner. *J Gen Virol* **85**, 959–969.

Takigawa, Y., Nagano-Fujii, M., Deng, L., Hidajat, R., Tanaka, M., Mizuta, H. & Hotta, H. (2004). Suppression of hepatitis C virus replicon by RNA interference directed against the NS3 and NS5B regions of the viral genome. *Microbiol Immunol* **48**, 591–598.

Tong, M. J., El-Farra, N. S., Reikes, A. R. & Co, R. L. (1995). Clinical outcomes after transfusion-associated hepatitis C. *N Engl J Med* **332**, 1463–1466.

Wang, F., Yoshida, I., Takamatsu, M., Ishido, S., Fujita, T., Oka, K. & Hotta, H. (2000). Complex formation between hepatitis C virus core protein and p21Waf1/Cip1/Sdi1. *Biochem Biophys Res Commun* **273**, 479–484.

Wang, H.-W., Sharp, T. V., Koumi, A., Koentges, G. & Boshoff, C. (2002). Characterization of an anti-apoptotic glycoprotein encoded by Kaposi's sarcoma-associated herpesvirus which resembles a spliced variant of human survivin. *EMBO J* **21**, 2602–2615.

Wölk, B., Sansonno, D., Kräusslich, H.-G., Dammacco, F., Rice, C. M., Blum, H. E. & Moradpour, D. (2000). Subcellular localization, stability, and *trans*-cleavage competence of the hepatitis C virus NS3-NS4A complex expressed in tetracycline-regulated cell lines. *J Virol* **74**, 2293–2304.

Zhu, N., Ware, C. F. & Lai, M. M. (2001). Hepatitis C virus core protein enhances FADD-mediated apoptosis and suppresses TRADD signaling of tumor necrosis factor receptor. *Virology* **283**, 178–187.

Journal of General Virology (2006), 87, 1703–1713 DOI 10.1099/vir.0.81735-0

NS3 protein of *Hepatitis C virus* associates with the tumour suppressor p53 and inhibits its function in an NS3 sequence-dependent manner

Lin Deng,[1] Motoko Nagano-Fujii,[1] Motofumi Tanaka,[1,2] Yuki Nomura-Takigawa,[1] Masanori Ikeda,[3] Nobuyuki Kato,[3] Kiyonao Sada[1] and Hak Hotta[1]

Correspondence
Hak Hotta
hotta@kobe-u.ac.jp

[1,2]Divisions of Microbiology[1] and Gastroenterological Surgery[2], Kobe University Graduate School of Medicine, Kobe 650-0017, Japan

[3]Department of Molecular Biology, Okayama University Graduate School of Medicine and Dentistry, Okayama 700-8558, Japan

The N-terminal 198 residues of NS3 (NS3-N) of *Hepatitis C virus* (HCV) subtype 1b obtained from 29 patients, as well as full-length NS3 (NS3-Full), were analysed for their subcellular localization, interaction with the tumour suppressor p53 and serine protease activity in the presence and absence of the viral cofactor NS4A. Based on the subcellular-localization patterns in the absence of NS4A, NS3-N sequences were classified into three groups, with each group exhibiting either dot-like, diffuse or a mixed type of localization. Chimeric NS3-Full sequences, each consisting of an individual NS3-N and a shared C-terminal sequence, showed the same localization patterns as those of the respective NS3-N. Site-directed mutagenesis experiments revealed that a single or a few amino acid substitutions at a particular position(s) of NS3-N altered the localization pattern. Interestingly, NS3 of the dot-like type, either NS3-N or NS3-Full, interacted with p53 more strongly than that of the diffuse type, in both the presence and the absence of NS4A. Moreover, NS3-N of the dot-like type suppressed *trans*-activating activity of p53 more strongly than that of the diffuse type. Serine protease activity did not differ significantly between the two types of NS3. In HCV RNA replicon-harbouring cells, physical interaction between NS3 and p53 was observed consistently and p53-mediated transcriptional activation was suppressed significantly compared with HCV RNA-negative control cells. Our results collectively suggest the possibility that NS3 plays an important role in the hepatocarcinogenesis of HCV by interacting differentially with p53 in an NS3 sequence-dependent manner.

Received 5 December 2005
Accepted 30 January 2006

INTRODUCTION

Chronic, persistent infection with *Hepatitis C virus* (HCV) often leads to liver cirrhosis and hepatocellular carcinoma (HCC) (Saito *et al.*, 1990). However, the exact mechanisms of HCV-associated pathogenesis and carcinogenesis are largely unknown.

HCV possesses a single-stranded, positive-sense RNA genome of 9·6 kb, which encodes a polyprotein of approximately 3000 aa. The polyprotein is processed into at least 10 structural and non-structural (NS) viral proteins by cellular and viral proteases (Reed & Rice, 2000). One of the viral proteases, the NS3 serine protease, has become a research focus, as it is indispensable for virus replication and, therefore, would be a good target for antiviral drugs. The serine protease is encoded in the N-terminal portion of NS3 and is responsible for cleavage at the NS3/4A, NS4A/4B, NS4B/5A and NS5A/5B junctions. NS4A, a cofactor for NS3, stabilizes it to augment its serine protease activity, being virtually essential for complete cleavage of the HCV polyprotein (Reed & Rice, 2000). The C-terminal portion of NS3 possesses the NTPase/helicase activity (Kim *et al.*, 1995), which is essential for viral RNA replication.

In addition to its key role in the life cycle of HCV, possible involvement of NS3 in viral persistence and hepatocarcinogenesis has been studied. For example, NS3 was reported to transform NIH3T3 (Sakamuro *et al.*, 1995) and rat fibroblast (Zemel *et al.*, 2001) cells. We also demonstrated that NIH3T3 cells constitutively expressing C-terminally truncated NS3 (aa 1–433) were more resistant to actinomycin D-induced apoptosis than control cells (Fujita *et al.*, 1996). It was also reported that NS3 could block transforming growth factor-β/Smad3-mediated apoptosis (Cheng *et al.*,

Supplementary figures showing subcellular-localization patterns and a sequence alignment are available in JGV Online.

2004). Moreover, the NS3–4A complex was shown to suppress beta interferon (IFN-β) induction by inhibiting retinoic acid-inducible gene I-mediated activation of IFN regulatory factor 3, counteracting innate immune responses to help establish persistent HCV infection (Foy *et al.*, 2003, 2005; Breiman *et al.*, 2005).

The tumour-suppressor protein p53 functions principally to control cell-cycle arrest and apoptosis upon various cellular stresses, ensuring completion of DNA repair and the integrity of the genome (Levine, 1997). It has been documented that oncogenic viral proteins, such as papillomavirus E6 (Münger & Howley, 2002; Longworth & Laimins, 2004), adenovirus E1B 55K (Martin & Berk, 1998), simian virus 40 large T antigen (Sheppard *et al.*, 1999) and hepatitis B virus X protein (Truant *et al.*, 1995), inhibit p53-mediated apoptosis via interacting with p53. In the case of HCV, NS5A (Lan *et al.*, 2002) and core protein (Kao *et al.*, 2004) were reported to suppress p53-dependent apoptosis. Our previous studies showed that NS3 colocalized with p53 in the nucleus (Ishido *et al.*, 1997; Muramatsu *et al.*, 1997) and that they formed a complex through an N-terminal portion of NS3 (aa 29–174) and a C-terminal portion of p53 (Ishido & Hotta, 1998). In a clinical setting, we found a strong correlation between HCC and predicted secondary structure of an N-terminal portion of NS3 (Ogata *et al.*, 2003). These observations prompted us to investigate the possible correlation between NS3 sequence diversity and p53 interaction. We report here that subcellular localization of NS3 and its interaction with p53 vary with different NS3 sequences.

METHODS

Plasmid construction. cDNA fragments encoding the N-terminal 198 residues of NS3 (NS3-N; aa 1–198) of HCV subtype 1b (HCV-1b) isolates were described previously (Ogata *et al.*, 2002, 2003). *Bam*HI and *Hin*dIII recognition sites were introduced by PCR into the 5′ and 3′ ends of the cDNAs, respectively. The cDNAs were digested with *Bam*HI and *Hin*dIII and subcloned into pcDNA3.1/*Myc*-His(−)C (Invitrogen). A single point mutation(s) was introduced into some plasmids by using a QuikChange site-directed mutagenesis kit (Stratagene). Expression plasmids for Myc-tagged full-length NS3 (NS3-Full) of different HCV isolates, MKC1a, M-H05-5, M-45, M-H17-2 and M-42, were reported elsewhere (Hidajat *et al.*, 2005). To express NS3–4A *in cis*, the corresponding region was amplified from pTMns2-5B/810-2721 (Muramatsu *et al.*, 1997) and subcloned into pcDNA3.1/*Myc*-His(−)C to generate pcDNA3.1/MKC1a/4A. Expression plasmids for chimeric NS3-Full flanked with NS4A were constructed, in which the N-terminal 355 residues were derived from M-H05-5 or M-H17-2, whereas the C-terminal 330 residues were derived from MKC1a/4A. They were designated pcDNA3.1/M-H05-5/4A and pcDNA3.1/M-H17-2/4A. The NS3 sequences were subcloned also into pSG5 (Stratagene).

An *Eco*RI fragment encoding full-length NS4A was obtained from pBSns4A (Muramatsu *et al.*, 1997) and subcloned into pcDNA3.1/*Myc*-His(−)C and pSG5. Myc-tagged NS4A was amplified from pFK5B/2884Gly (a kind gift from Dr R. Bartenschlager, University of Heidelberg, Heidelberg, Germany) and subcloned into pEF1/*Myc*-His (Invitrogen). An expression plasmid for Myc-tagged NS4B was reported elsewhere (Tanaka *et al.*, 2006). To express a polyprotein consisting of full-length NS5A and C-terminally truncated NS5B (NS5A/5BΔC; aa 1973–2720 of the entire HCV polyprotein), the corresponding region was amplified from pTMns2-5B/810-2721 (Muramatsu *et al.*, 1997) and subcloned into pTM1 (Moss *et al.*, 1990).

An *Xho*I fragment encoding full-length wild-type p53 was obtained from pBSp53/1-393 (Ishido & Hotta, 1998) and subcloned into pcDNA3.1/*Myc*-His(−)C. pSG5/p53 (Florese *et al.*, 2002) was also used.

All of the plasmid constructs were verified for the correct sequence by DNA sequencing.

Cell culture and protein expression. Huh-7 and HeLa cells were cultured in Dulbecco's modified Eagle's medium supplemented with 10% fetal calf serum. For protein expression, cells were infected with a recombinant vaccinia virus expressing T7 RNA polymerase (vTF7-3) (Fuerst *et al.*, 1986). After 1 h, the cells were transfected with the expression plasmids by using Lipofectin reagent (Invitrogen). After cultivation overnight, the proteins expressed in the cells were analysed by co-immunoprecipitation, immunoblot and immunofluorescence techniques, as described below. For the luciferase reporter assay, Huh-7 cells were transfected with plasmids by using Fugene 6 transfection reagent (Roche) and cultivated for 24 h before analysis.

Huh-7 cells stably harbouring an HCV subgenomic RNA replicon were prepared as described previously (Taguchi *et al.*, 2004; Hidajat *et al.*, 2005), using pFK5B/2884Gly (Lohmann *et al.*, 2001). Cured Huh-7 cells were prepared by treating the HCV replicon-harbouring cells with IFN-α (1000 IU ml^{-1}) for 1 month (Hidajat *et al.*, 2005). Full-length HCV RNA-harbouring Huh-7 cells, designated O, and IFN-cured cells, designated Oc, were described previously (Ikeda *et al.*, 2005).

Indirect immunofluorescence. Cells expressing Myc-tagged NS3 were fixed with methanol at −20 °C for 20 min and incubated with an anti-Myc mouse mAb (9E10; Santa Cruz Biotech) for 1 h at room temperature. In some experiments, an anti-NS3 mouse mAb (4A-3; a kind gift from Dr I. Fuke, Research Foundation for Microbial Diseases, Osaka University, Kagawa, Japan) was used to detect NS3-Full. An anti-haemagglutinin (HA) mouse mAb (HA.11; Covance Inc.) served as a control IgG. After being washed with PBS, the cells were incubated with fluorescein isothiocyanate-conjugated goat anti-mouse IgG (MBL) and observed under a laser-scanning confocal microscope (LSM510 version 3.0; Carl Zeiss).

Immunoprecipitation and immunoblotting. Cells expressing NS3 (Myc-tagged or untagged) and p53 were lysed in a stringent RIPA buffer containing 10 mM Tris/HCl (pH 7·5), 150 mM NaCl, 1 mM EDTA, 0·1% SDS, 1% NP-40, 0·1% sodium deoxycholate and protease inhibitor cocktail (Roche) for 30 min on ice. The cell lysates were centrifuged and the supernatants were cleared by mixing with 0·25 μg normal rabbit IgG (Santa Cruz Biotech) and 15 μl protein A–Sepharose beads (Amersham Biosciences) at 4 °C for 30 min on a rotator to reduce non-specific precipitation. The cleared lysates were incubated with anti-p53 rabbit polyclonal antibody (FL-393; Santa Cruz Biotech) at 4 °C for 1 h and subsequently with 15 μl protein A–Sepharose beads for another 1 h. The beads were washed six times with RIPA buffer and the immunoprecipitates were separated by SDS-PAGE and analysed by immunoblotting (see below). To analyse the interaction of NS3 expressed in the context of HCV RNA replication with p53, the HCV subgenomic or full-length RNA replicon-harbouring cells were lysed in a mild RIPA buffer without 0·1% SDS and 0·1% sodium deoxycholate. The lysates were subjected to immunoprecipitation analysis in the same way as described above, except that the beads were washed with PBS instead of RIPA buffer. Anti-FLAG rabbit polyclonal antibody (Sigma) served as a control.

Immunoblot analysis was performed as described previously (Hidajat *et al.*, 2005). Mouse mAbs against Myc (9E10), NS3, NS4A (S4-13; a kind gift from Dr I. Fuke) and p53 (Ab-1; Calbiochem) were used as primary antibodies and peroxidase-labelled goat anti-mouse IgG (MBL) as a secondary antibody. The protein bands were visualized by an enhanced chemiluminescence method (ECL; Amersham Biosciences) and the intensity of the bands was quantified by using NIH Image 1.61.

Luciferase reporter assay. p53-Luc (Stratagene), which contains the *Photinus pyralis* (firefly) luciferase reporter gene driven by a basic promoter element plus an inducible *cis*-enhancer element, containing 14 repeats of the p53-binding sequence (TGCCTGGACTTGCCTGG), was used as a reporter plasmid. pRL-SV40 (Promega), which expresses *Renilla* luciferase, was used as a control plasmid to check transfection efficiency. Huh-7 cells prepared in a 24-well tissue-culture plate were transfected transiently with p53-Luc (10 ng), pRL-SV40 (1 ng), pSG5/p53 (5 ng) and pSG5/NS3-N or pSG5/NS3-Full (250 ng) in the absence or presence of pSG5/NS4A (75 ng). After 24 h, the cells were harvested and a luciferase assay was performed by using the Dual-Luciferase Reporter Assay system (Promega), as described previously (Kadoya *et al.*, 2005). Firefly and *Renilla* luciferase activities were measured by using a Luminescencer-JNR AB-2100 (Atto). Firefly luciferase activity was normalized to *Renilla* luciferase activity for each sample.

NS3 serine protease activity. HeLa cells transiently coexpressing NS5A/5BΔC and Myc-tagged NS3 were lysed in gel-loading buffer containing 50 mM Tris/HCl (pH 6·8), 5 % 2-mercaptoethanol, 2 % SDS, 0·1 % bromophenol blue and 10 % glycerol. The lysates were separated by SDS-PAGE and analysed by immunoblotting using anti-NS5A (8926; a kind gift from Dr I. Fuke) and anti-Myc antibodies (9E10). Intensity of the bands corresponding to the cleaved NS5A and the uncleaved NS5A/5BΔC was measured. Arbitrary units of serine protease activity of each NS3 were calculated by the following formula: protease activity (arbitrary units) = NS5A/(NS5A/5BΔC + NS5A).

RESULTS

NS3-N sequences of different HCV-1b isolates exhibit distinct subcellular-localization patterns in a sequence-dependent manner

We first examined the subcellular localization of NS3-N in HeLa cells. As shown in Fig. 1(a), we noticed three distinct patterns of NS3-N localization: (i) dot-like staining in both the cytoplasm and the nucleus, (ii) diffuse staining predominantly in the cytoplasm and (iii) a mixed pattern of the former two. Of the 29 HCV-1b isolates tested, 15 (52 %) exhibited exclusively the dot-like staining, nine (31 %) the diffuse staining and the remaining five (17 %) the mixed pattern. The subcellular-localization patterns of four NS3-N sequences each from the dot-like, diffuse and mixed staining groups are also shown in Supplementary Fig. S1 (available in JGV Online). Similar results were obtained when NS3-N sequences were expressed in Huh-7 cells (data not shown), suggesting that the distinct localization patterns among different NS3 sequences are not restricted to a particular cell line.

In order to see which amino acid residue(s) affected the subcellular localization of NS3, we determined the sequences of all 29 isolates. Some of the sequences showing the typical localization patterns, along with a standard sequence, are shown in Fig. 1(b). For more information, the sequences of all 29 isolates are shown in Supplementary Fig. S2 (available in JGV Online). We did not find any common amino acid residue(s) that was/were associated with a particular localization pattern. We noticed, however, that a substitution at position 17 or 18 (Ile to Val) was observed with some NS3 sequences of the dot-like pattern, but not with any NS3 sequences of the other localization patterns. Also, a substitution(s) at positions 150–153 (Val to Ala, Ile to Val) appeared to be more frequent in NS3 sequences of the dot-like pattern. To examine the possible importance of those substitutions, we introduced a point mutation(s) to some NS3-N of the dot-like pattern (Fig. 1c). Introduction of two point mutations at positions 18 and 153 into NS3-N of isolate H05-5 did not alter the localization pattern. However, introduction of an additional two point mutations at positions 80 and 122 altered the localization pattern significantly, with the majority of the cells exhibiting the typical diffuse staining. Similarly, introduction of two mutations at positions 17 and 86, but not of either one alone, into NS3-N of isolate 45 altered the localization pattern from dot-like to diffuse staining. As for isolate 63, a single point mutation at position 150 alone was enough to change the localization pattern of NS3-N. These results suggest that residues at positions 17 or 18, 80–86 and/or 150–153 play an important role in determining the localization pattern of some, but not all, NS3 sequences.

NS3-N binds to p53 and inhibits its *trans*-activating activity in an NS3 sequence-dependent manner

We previously reported that a region near the N terminus of NS3 (aa 29–174) was involved in complex formation with p53 (Ishido & Hotta, 1998). In this study, we examined whether interaction between NS3-N and p53 differs with different NS3-N sequences. We selected two NS3-N sequences each from the dot-like (H05-5 and 45) and diffuse (H17-2 and 42) staining groups. Co-immunoprecipitation analysis demonstrated that NS3-N of isolate H05-5 interacted with p53 most strongly, followed by that of isolate 45, both in the absence (Fig. 2a) and the presence (Fig. 2b) of NS4A. On the other hand, NS3-N of the diffuse-staining group interacted only weakly with p53. The specificity of the interaction between NS3-N and p53 was confirmed by a control experiment, in which neither NS4A nor NS4B bound to p53 under the same experimental conditions (Fig. 2c, left and centre panels). The specificity of the NS3–p53 interaction was also secured by another control experiment using an irrelevant (anti-FLAG) antibody (Fig. 2c, right panel).

Next, we examined the possible effect of NS3-N on p53 function. The plasmid p53-Luc harbours 14 copies of p53-responsive elements and a minimum promoter upstream of a luciferase gene, and is used to monitor p53-dependent transcriptional activity. Interestingly, NS3-N of H05-5 and that of isolate 45 inhibited p53-dependent transcription of the luciferase gene strongly and moderately, respectively

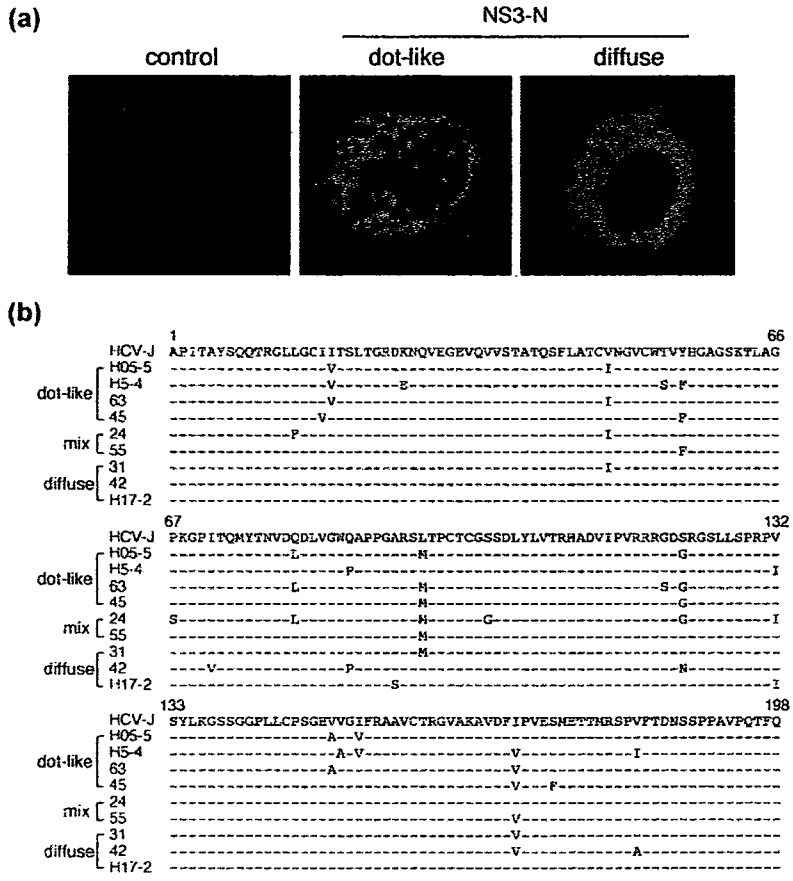

Fig. 1. Distinct subcellular-localization patterns of NS3-N of different HCV-1b isolates and the alignment of their sequences. (a) NS3-N was expressed in HeLa cells using a vaccinia virus–T7 hybrid expression method. Typical immunofluorescence images of the dot-like (middle panel) and diffuse (right panel) localization patterns of NS3-N of isolates H05-5 and H17-2, respectively, are shown. As a control, cells expressing NS3-N of H05-5 (left panel) were stained with an irrelevant (anti-HA) antibody. (b) Sequence alignment of representative sequences of each of the staining groups along with a standard sequence of the HCV-J strain (top). Dashes indicate residues identical to those of HCV-J. The numbers along the sequence indicate amino acid positions. (c) Identification of residues that alter the localization patterns of NS3-N of the isolates H05-5, 45 and 63. Substituted residues at the indicated positions are shown.

(Fig. 2d). On the other hand, no inhibition was observed with NS3-N of isolate 42 and even a slight increase in p53-dependent transcription was observed with NS3-N of H17-2.

NS3 forms a stable complex with its cofactor NS4A, which may counteract the NS3-mediated inhibitory action of p53-dependent transcription. In fact, we observed that inhibition of the p53-dependent transcription by NS3-N of the H05-5 isolate was alleviated to some extent, but not completely, by coexpression of NS4A (Fig. 2e).

To further test the possibility that the alteration in the localization pattern of NS3-N affects its interaction with p53, we compared NS3-N of H05-5 with its point mutant H05-5/mut (Fig. 1c) in terms of their p53-binding abilities and inhibitory effects on p53-dependent transcription. The result obtained demonstrated that NS3-N of H05-5/mut, which showed diffuse localization, had weaker p53-binding capacity (Fig. 3a) and exerted weaker inhibition on p53-dependent transcription (Fig. 3b) compared with NS3-N of the parental H05-5, showing the dot-like localization. Similar results were obtained with isolates 45 and 63 and their point mutants (data not shown). Our results thus suggest that NS3-N of the dot-like localization pattern interacts with p53 more strongly and inhibits p53-mediated transcriptional activation more efficiently than that of the diffuse localization.

NS3-Full sequences exhibit the same subcellular-localization patterns as those of NS3-N sequences derived from the same isolates and interact differentially with NS4A and p53 in an NS3 sequence-dependent manner

As shown above, NS3-N exhibited a distinct subcellular-localization pattern in a sequence-dependent manner when expressed alone (see Fig. 1). Moreover, we have reported that NS3, either NS3-N or NS3-Full, enters the nucleus when

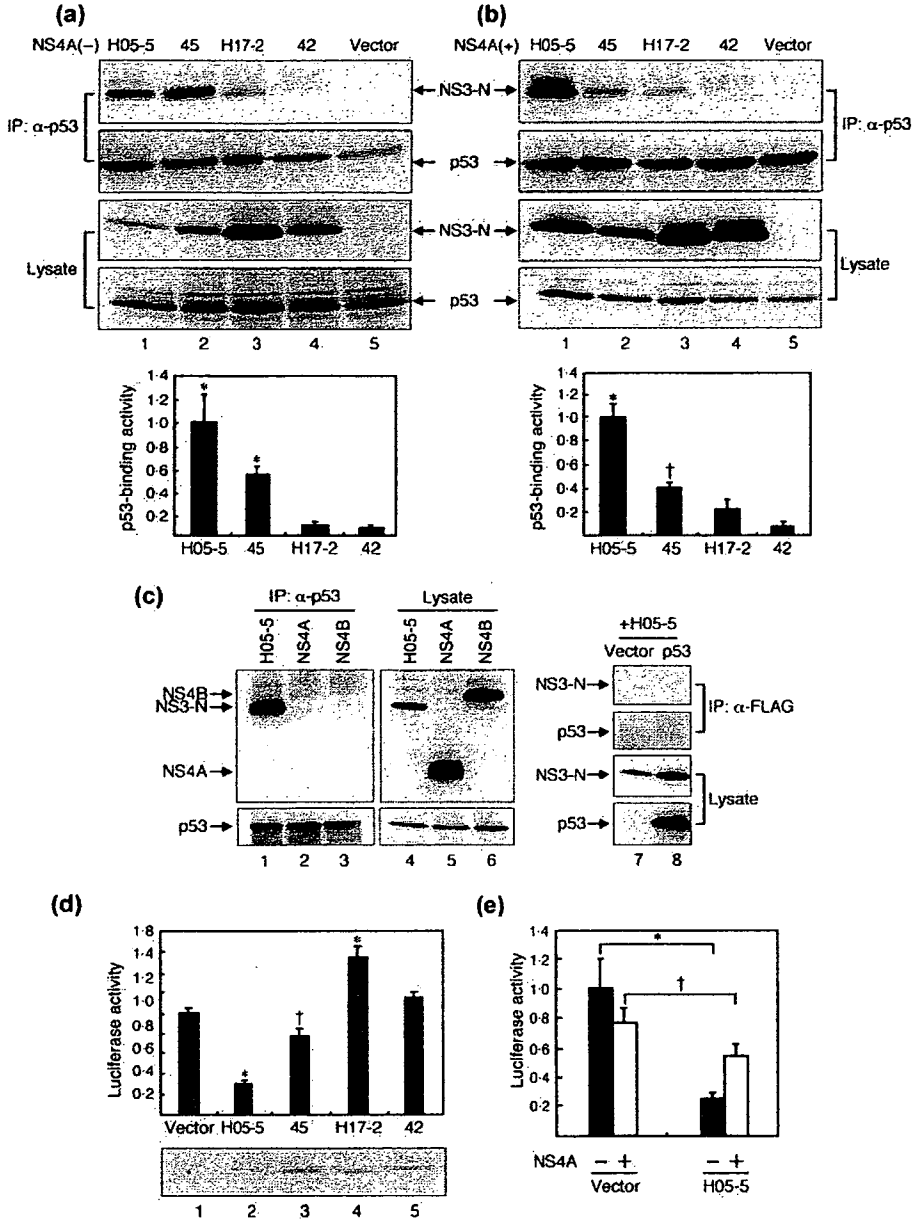

Fig. 2. Physical and functional interactions between NS3-N and p53 in an NS3 sequence-dependent manner. NS3-N and p53 were coexpressed in the absence (a) and presence (b) of NS4A. Cells that did not express NS3-N served as a control. Cell lysates were immunoprecipitated by using an anti-p53 antibody and probed by immunoblotting using an anti-Myc antibody to detect NS3-N (top row). Efficient immunoprecipitation of p53 was verified (second row). Lysates were probed directly (without being immunoprecipitated with anti-p53 antibody) with anti-Myc and anti-p53 antibodies, respectively, to verify comparable expression levels of NS3-N (third row) and p53 (bottom row). The intensity of the bands for NS3-N co-immunoprecipitated with p53 was quantified and normalized to the expression levels of NS3-N in the lysates. Filled columns and bars represent mean ± SD obtained from three independent experiments. The p53-binding intensity of NS3-N of the isolate H05-5 was expressed as 1·0. *$P<0·01$; †$P<0·05$, compared with isolate 42. (c) Cells expressing Myc-tagged H05-5, NS4A or NS4B together with p53 were analysed by immunoprecipitation using an anti-p53 antibody (left). Lysates were probed directly with anti-Myc and anti-p53 antibodies, respectively (middle). Cells expressing Myc-tagged H05-5 with or without p53 were analysed by immunoprecipitation using an irrelevant (anti-FLAG) antibody (right). (d) Inhibition of p53-dependent transcription by NS3-N in an NS3 sequence-dependent manner. pSG5-based NS3-N expression plasmids were each co-transfected with pSG5/p53, p53-Luc and pRL-SV40 in Huh-7 cells and cultivated for 24 h. Firefly luciferase activity was measured and normalized to *Renilla* luciferase activity. The luciferase activity in the control cells without NS3-N expression was expressed arbitrarily as 1·0. Results are shown as mean ± SD from three independent experiments. *$P<0·01$; †$P<0·05$, compared with the control. Expression levels of NS3-N in the cells are shown at the bottom. (e) Inhibition of p53-dependent transcription by NS3-N of H05-5 in the absence (filled bars) and presence (open bars) of NS4A. Results are shown as mean ± SD from three independent experiments. *$P<0·01$; †$P<0·05$, compared with the control.

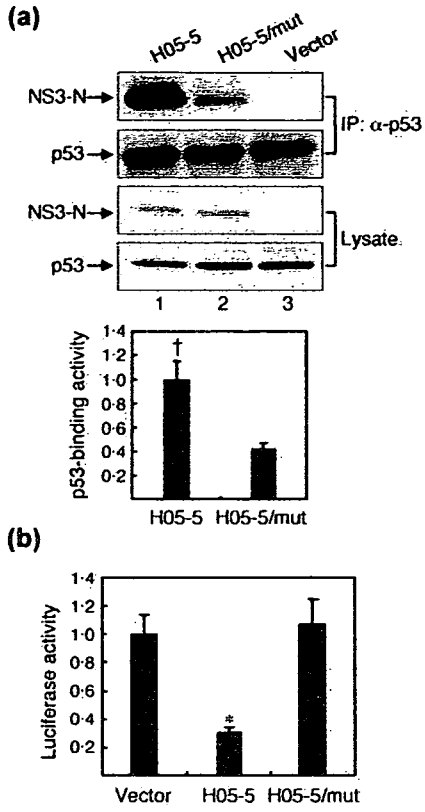

Fig. 3. Comparison between NS3-N of the isolate H05-5 and its point mutant H05-5/mut in their capacity to interact with p53. (a) Physical interaction with p53 was analysed as described in the legend to Fig. 2(a). Filled columns and bars represent mean ± SD obtained from three independent experiments. The p53-binding intensity of NS3-N of H05-5 was expressed as 1·0. †$P<0·05$. (b) Functional interaction with p53 was analysed as described in the legend to Fig. 2(c). Results are shown as mean ± SD from three independent experiments. *$P<0·01$ compared with H05-5/mut.

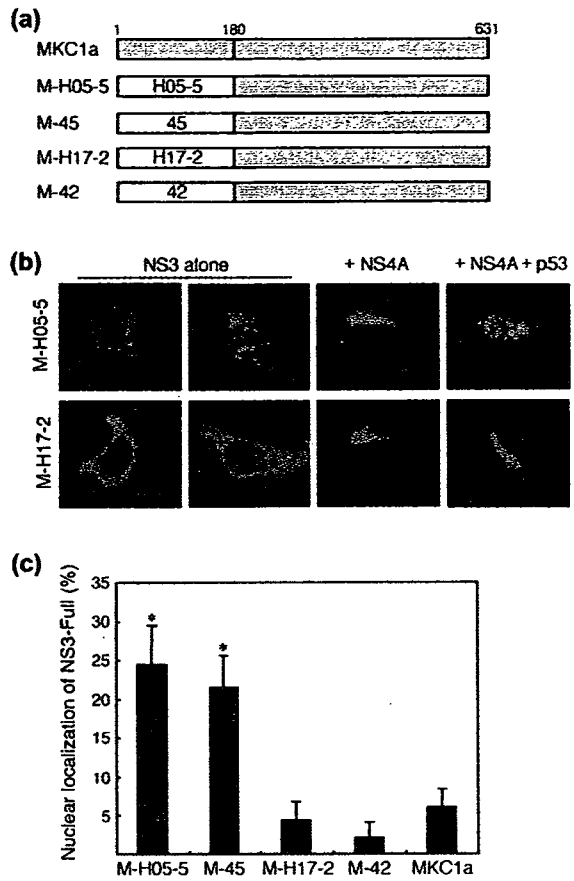

Fig. 4. Subcellular localization of NS3-Full in the presence and absence of NS4A and p53. (a) Schematic representation of NS3-Full of different sequences. The N-terminal 180 residues are derived from clinical isolates (H05-5, H17-2, 42 and 45) and the C-terminal 451 residues from the parental MKC1a strain. (b) Subcellular localization of M-H05-5 (upper) and M-H17-2 (lower) when expressed alone, when coexpressed with NS4A and when coexpressed with NS4A and p53. The cells were stained with either anti-NS3 (left panels) or anti-Myc antibody (left-middle, right-middle and right panels). (c) Percentage of cells with nuclear accumulation of NS3-Full when coexpressed with NS4A and p53. *$P<0·01$ compared with M-42.

coexpressed with p53 and that the p53-mediated nuclear localization of NS3 is inhibited by NS4A in an NS3 sequence-dependent manner (Muramatsu *et al.*, 1997). Therefore, we examined the subcellular-localization patterns of NS3-Full of different sequences, both when expressed alone and when coexpressed with p53 and/or NS4A. The NS3-Full sequences tested differ from each other only in the N-terminal 180 residues that are derived from the clinical isolates, with the C-terminal 451 residues being shared among all the strains tested (Fig. 4a; Hidajat *et al.*, 2005). When expressed alone, NS3-Full of all four strains exhibited the same subcellular-localization patterns as those of NS3-N of the same strains (Fig. 4b; data not shown for M-45 and M-42). When coexpressed with NS4A, NS3-Full was localized in the cytoplasm, especially in perinuclear regions, regardless of the strain tested. Interestingly, when p53 was additionally coexpressed with NS4A, NS3-Full of the dot-like type (M-H05-5 and M-45) showed an increased tendency to accumulate in the nucleus together with p53 (Fig. 4b), with nearly 25 % of the cells exhibiting nuclear localization of NS3 (Fig. 4c). Concomitant expression of NS4A in the cytoplasm of the same cells was confirmed by double-staining immunofluorescence analysis (data not shown), the result being consistent with our previous observation (Ishido *et al.*, 1997). On the other hand, NS3-Full of the diffuse type (M-H17-2, M-42 and MKC1a) was localized almost exclusively in the cytoplasm together with NS4A. Similar results were obtained when NS3-N sequences of different isolates were coexpressed with p53 and/or NS4A (data not shown).

We then tested complex formation between NS3-Full of the five different sequences and p53. The results demonstrated clearly that NS3-Full of the dot-like type (M-H05-5 and

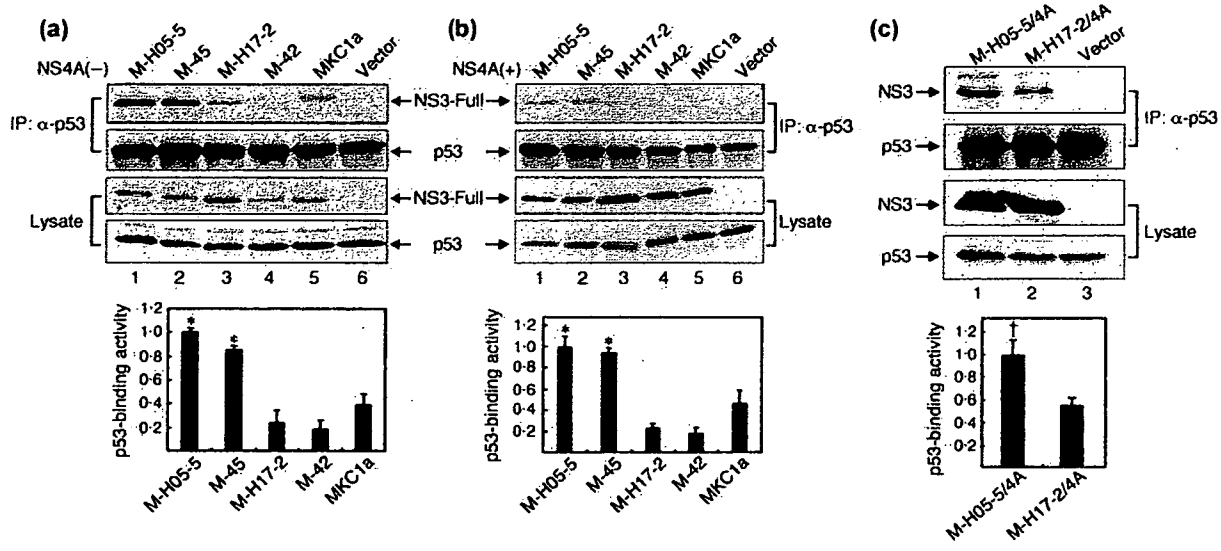

Fig. 5. Physical interaction between NS3-Full and p53 in an NS3 sequence-dependent manner. NS3-Full of different strains in the absence (a) and presence of NS4A coexpression *in trans* (b) were analysed as described in the legend to Fig. 2(a). Filled columns and bars represent mean ± SD obtained from three independent experiments. The p53-binding intensity of M-H05-5 was expressed as 1·0. *$P<0·01$ compared with M-42. (c) M-H05-5/4A and M-H17-2/4A (NS3–4A coexpression *in cis*) were analysed as described in the legend to Fig. 2(a), except that anti-NS3 antibody was used instead of anti-Myc antibody. Filled columns and bars represent mean ± SD obtained from three independent experiments. The p53-binding intensity of M-H05-5/4A was expressed as 1·0. †$P<0·05$ compared with M-H17-2/4A.

M-45) interacted with p53 more strongly than that of the diffuse type (M-H17-2, M-42 and MKC1a), both in the absence and presence of NS4A (Fig. 5a, b). In this connection, it should be noted that the interaction between NS3-Full and p53 was weaker in the presence of NS4A than in its absence. We also examined the interaction of NS3 with p53 when full-length NS3–4A was expressed *in cis*, where NS3–4A complex formation occurs more efficiently than *in trans*. The results demonstrated that M-H05-5/4A interacted with p53 more strongly than did M-H17-2/4A (Fig. 5c), again suggesting NS3 sequence-dependent interaction with p53.

NS3 binds to p53 and inhibits its *trans*-activating activity in HCV RNA replicon-harbouring cells

In order to determine whether NS3 expressed in the context of HCV replication interacted with p53, we used Huh-7 cells harbouring an HCV subgenomic RNA replicon and examined physical and functional interactions between NS3 and p53. Co-immunoprecipitation analysis revealed that NS3 interacted physically with p53 in HCV subgenomic RNA replicon-harbouring cells, albeit with much lower efficiency than in the plasmid-based expression system (Fig. 6a). We also used the full-length HCV RNA replicon, whose NS3 is detected more strongly than that of the subgenomic RNA replicon by the anti-NS3 mAb used in this study. The result demonstrated that NS3 expressed in the context of HCV RNA replication interacted efficiently with p53, irrespective of whether p53 was expressed ectopically or endogenously (Fig. 6b). The specificity of the interaction between NS3 and p53 was confirmed by the lack of interaction between NS4A and p53 in HCV subgenomic RNA-harbouring cells (Fig. 6c). Next, we compared *trans*-activating activity of p53 between HCV RNA replicon-harbouring cells and the HCV-negative controls (parental and cured Huh-7 cells). We observed that p53-dependent transcription was suppressed significantly in cells harbouring an HCV RNA replicon, either subgenomic or full-length, compared with the parental and cured Huh-7 cells (Fig. 6d, e). These results suggest collectively that NS3 expressed in the context of HCV replication inhibits p53 function.

Serine protease activity of NS3-Full in the absence and presence of NS4A

The N-terminal portion of NS3 possesses a serine protease activity that can cleave the NS5A/5B junction even in the absence of NS4A (Lin *et al.*, 1994). By using NS5A/5BΔC as a substrate, we compared the serine protease activities of NS3-Full of different subcellular-localization patterns. A tendency was noted that, in the absence of NS4A, NS3-Full of the dot-like type showed slightly weaker protease activity than that of the diffuse type (Fig. 7). This difference might be attributable, at least partly, to the fact that NS5A/5BΔC was localized diffusely in the cytoplasm (Kim *et al.*, 1999; Mottola *et al.*, 2002; data not shown) and, therefore, could be recognized more easily by NS3 of the same localization pattern than by NS3 of the other type. In the presence of

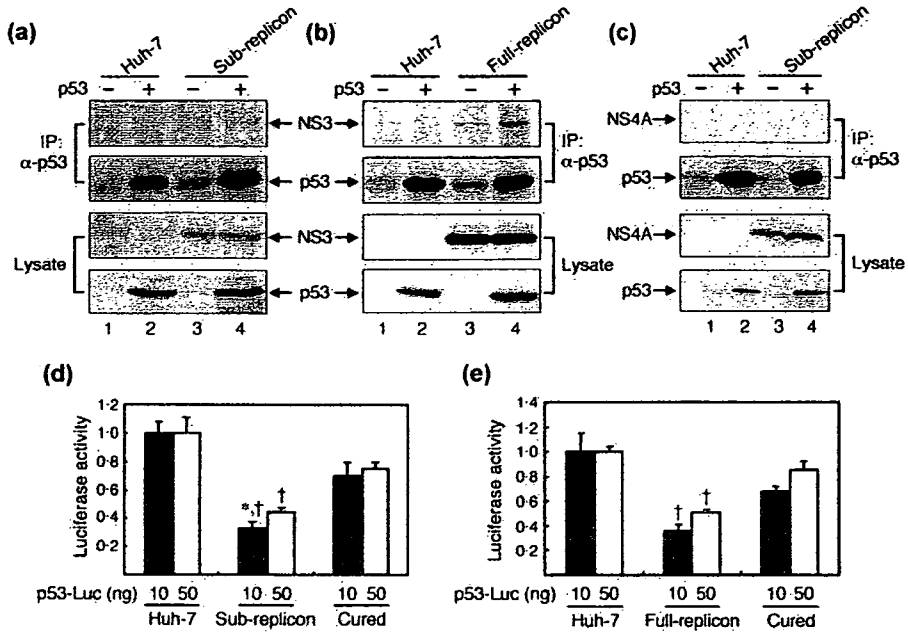

Fig. 6. Physical and functional interactions between NS3 and p53 in HCV RNA replicon-harbouring cells. p53 was expressed ectopically in Huh-7 cells harbouring either HCV subgenomic (a) or full-length (b) RNA replicon and the parental Huh-7 cells by using a vaccinia virus–T7 hybrid expression method. Cell lysates were analysed as described in Methods. (c) The lack of interaction between NS4A and p53 in HCV subgenomic RNA replicon-harbouring Huh-7 cells was confirmed. Inhibition of p53-dependent transcription in Huh-7 cells harbouring either HCV subgenomic (d) or full-length (e) RNA replicon. Cells were co-transfected with p53-Luc (10 and 50 ng, filled and open bars, respectively), pSG5/p53 (10 ng) and pRL-SV40 (1 ng) as an internal control. After 24 h, firefly luciferase activity was measured and normalized to *Renilla* luciferase activity. Luciferase activities in the parental Huh-7 cells were expressed arbitrarily as 1·0. Cured cells also served as a control. Results are shown as mean ± SD from three independent experiments. $^*P<0{\cdot}01$; $\dagger P<0{\cdot}05$, compared with the parental and cured Huh-7 cells.

NS4A, on the other hand, all of the NS3-Full sequences, which accumulated at a perinuclear region of the cytoplasm (see Fig. 4b), exhibited an enhanced and comparable degree of serine protease activity among the five strains (Fig. 7). Similar results were obtained when Huh-7 cells were used instead of HeLa cells (data not shown).

DISCUSSION

In the present study we demonstrated that, when expressed alone, NS3 of HCV-1b isolates, either NS3-N or NS3-Full, exhibited distinct subcellular-localization patterns, i.e. (i) dot-like staining both in the cytoplasm and the nucleus, (ii) diffuse staining predominantly in the cytoplasm and (iii) a mixed type, in a sequence-dependent manner (Figs 1 and 4). Although no significant correlation has been observed so far between the localization patterns of NS3 and the HCC status of the patients, it was interesting to find that NS3-N and NS3-Full of the dot-like staining pattern interacted with p53 more strongly than that of the diffuse-staining pattern (Figs 2a, 3a and 5a). Similar results were obtained when NS3 was coexpressed with NS4A (Figs 2b, 5b and 5c). We also observed that both NS3-N and NS3-Full of the dot-like staining pattern, but not those of the diffuse pattern, were more prone to colocalize with p53 in the nucleus even in the presence of NS4A (Fig. 4). Luciferase reporter analysis demonstrated that NS3-N of the dot-like type, but not that of the diffuse type, suppressed p53-dependent transcriptional activation significantly (Figs 2d and 3b).

When cells are exposed to a variety of stresses, p53 is induced to accumulate in the nucleus, where it functions as a transcription factor for cell-cycle regulators such as p21 (Levine, 1997). Our present results demonstrated that NS3-N of isolate H05-5 inhibited p53-dependent transcription of a reporter gene strongly (Figs 2d and 3b). We need to assess two possible mechanisms for the NS3-N-mediated p53 inhibition: NS3 might inhibit either p53 expression or p53 function itself. Our results showed that p53 expression levels were not altered significantly by NS3-N, irrespective of the localization patterns (Fig. 2a, b, bottom). Similar results that neither p53 mRNA nor protein levels were downregulated by NS3 were reported by Kwun *et al.* (2001). Overexpression of p53 was even observed in hepatocytes of some, if not all, HCV-infected patients (Loguercio *et al.*, 2003). It is likely, therefore, that NS3-N inhibits p53 function by interacting with it physically.

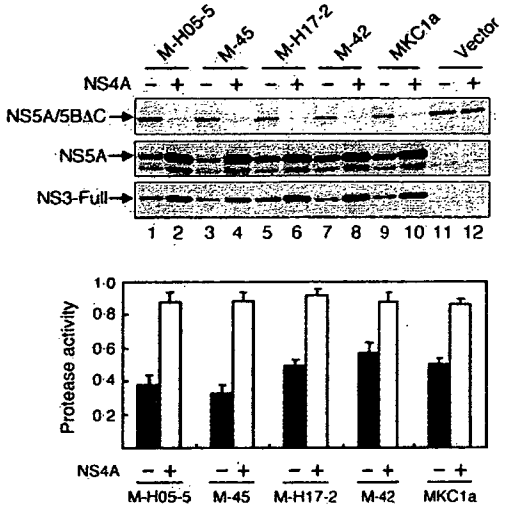

Fig. 7. Serine protease activity of NS3-Full in the absence and presence of NS4A. NS3-Full of different strains and NS5A/5BΔC were coexpressed in HeLa cells without (lanes with odd numbers) or with (lanes with even numbers) NS4A using a vaccinia virus–T7 hybrid expression method. Cell lysates were subjected to immunoblotting using anti-NS5A or anti-Myc antibody to detect NS5A/5BΔC (top), NS5A (middle) and NS3 (bottom). The intensity of the bands was quantified and arbitrary units of serine protease activity were calculated as described in Methods. Serine protease activities of NS3-Full in the absence (filled bars) and presence (open bars) of NS4A obtained from three independent experiments are shown.

We previously reported that a region of p53 near the C terminus (aa 301–360) was involved in complex formation with NS3 (Ishido & Hotta, 1998). This region includes the p53 oligomerization domain (aa 324–355) (Levine, 1997). It is known that the p53 tetramer binds to the p53-response element on promoter sequences most efficiently and, therefore, is most effective in *trans*-activation of its target genes (McLure & Lee, 1998; Weinberg *et al.*, 2004). Recently, it was reported that proteins of the S100 family disrupted p53 tetramerization via binding to its tetramerization domain (Fernandez-Fernandez *et al.*, 2005). Therefore, it is reasonable to assume that interaction of NS3-N with p53 interferes with its tetramer formation and DNA binding, thereby inhibiting p53-dependent transcriptional activation. It was also reported that a C-terminal portion of p53 (aa 364–393) negatively regulated its DNA-binding capacity (Müller-Tiemann *et al.*, 1998) and that the 14-3-3 proteins could associate with this region to counteract the negative regulation, which resulted in increased DNA binding of p53 (Waterman *et al.*, 1998). It is tempting to speculate that, by binding to a nearby region of p53, NS3-N may impair the association of 14-3-3 proteins with p53, which results in comparably decreased DNA binding of p53. Moreover, p53 is subject to post-translational modifications, including phosphorylation and acetylation, that affect p53 function (Appella & Anderson, 2001). Further study is needed to determine whether such p53 modification status is affected, either directly or indirectly, by NS3-N.

Consistent with the results obtained from transient-expression experiments, physical interaction between NS3 and p53 was also observed in Huh-7 cells harbouring either an HCV subgenomic or full-length RNA replicon, albeit to a smaller extent than in the transient-expression system (Fig. 6). It should be noted that NS3 expressed by the full-length RNA replicon is detected more strongly by the anti-NS3 antibody used in this study than that of the subgenomic RNA replicon. In HCV RNA replicon-harbouring cells, the HCV non-structural proteins are incorporated into the HCV RNA replication complex and, therefore, it is conceivable that only a minor fraction of NS3 is available for the interaction with p53. Nevertheless, p53-mediated transcriptional activation was suppressed significantly in HCV RNA replicon-harbouring cells compared with the controls (Fig. 6d, e). We must consider the possibility that not only NS3, but also other HCV proteins, are involved in the observed p53 inhibition. In fact, interaction between NS5A and p53 has been reported (Lan *et al.*, 2002; Qadri *et al.*, 2002).

In conclusion, our present results have demonstrated that NS3 of HCV-1b can be divided into three groups based on the subcellular-localization patterns and that NS3 of the dot-like localization pattern interacts with, and inhibits the function of, the tumour suppressor p53 more strongly than that of the diffuse type. The observed difference may account, at least partly, for a different degree of the oncogenic capacity of different HCV-1b isolates.

ACKNOWLEDGEMENTS

The authors are grateful to Dr I. Fuke, Research Institute for Microbial Diseases, Kan-Onji Branch, Kagawa, Japan, for providing anti-NS3, anti-NS4A and anti-NS5A mAbs. Thanks are also due to Dr R. Bartenschlager (University of Heidelberg, Heidelberg, Germany) for providing an HCV subgenomic RNA replicon (pFK5B/2884Gly). This study was supported in part by Grants-in-Aid for Scientific Research from the Ministry of Education, Culture, Sports, Science and Technology, the Japan Society for the Promotion of Science and the Ministry of Health, Labour and Welfare, Japan. This study was also carried out as part of the 21COE Program at Kobe University Graduate School of Medicine.

REFERENCES

Appella, E. & Anderson, C. W. (2001). Post-translational modifications and activation of p53 by genotoxic stresses. *Eur J Biochem* **268**, 2764–2772.

Breiman, A., Grandvaux, N., Lin, R., Ottone, C., Akira, S., Yoneyama, M., Fujita, T., Hiscott, J. & Meurs, E. F. (2005). Inhibition of RIG-I-dependent signaling to the interferon pathway during hepatitis C virus expression and restoration of signaling by IKKε. *J Virol* **79**, 3969–3978.

Cheng, P.-L., Chang, M.-H., Chao, C.-H. & Wu Lee, Y.-H. (2004). Hepatitis C viral proteins interact with Smad3 and differentially regulate TGF-β/Smad3-mediated transcriptional activation. *Oncogene* **23**, 7821–7838.

Fernandez-Fernandez, M. R., Veprintsev, D. B. & Fersht, A. R. (2005). Proteins of the S100 family regulate the oligomerization of p53 tumor suppressor. *Proc Natl Acad Sci U S A* **102**, 4735–4740.

Florese, R. H., Nagano-Fujii, M., Iwanaga, Y., Hidajat, R. & Hotta, H. (2002). Inhibition of protein synthesis by the nonstructural proteins NS4A and NS4B of hepatitis C virus. *Virus Res* **90**, 119–131.

Foy, E., Li, K., Wang, C., Sumpter, R., Jr, Ikeda, M., Lemon, S. M. & Gale, M., Jr (2003). Regulation of interferon regulatory factor-3 by the hepatitis C virus serine protease. *Science* **300**, 1145–1148.

Foy, E., Li, K., Sumpter, R., Jr & 8 other authors (2005). Control of antiviral defenses through hepatitis C virus disruption of retinoic acid-inducible gene-I signaling. *Proc Natl Acad Sci U S A* **102**, 2986–2991.

Fuerst, T. R., Niles, E. G., Studier, F. W. & Moss, B. (1986). Eukaryotic transient-expression system based on recombinant vaccinia virus that synthesizes bacteriophage T7 RNA polymerase. *Proc Natl Acad Sci U S A* **83**, 8122–8126.

Fujita, T., Ishido, S., Muramatsu, S., Itoh, M. & Hotta, H. (1996). Suppression of actinomycin D-induced apoptosis by the NS3 protein of hepatitis C virus. *Biochem Biophys Res Commun* **229**, 825–831.

Hidajat, R., Nagano-Fujii, M., Deng, L., Tanaka, M., Takigawa, Y., Kitazawa, S. & Hotta, H. (2005). Hepatitis C virus NS3 protein interacts with ELKS-δ and ELKS-α, members of a novel protein family involved in intracellular transport and secretory pathways. *J Gen Virol* **86**, 2197–2208.

Ikeda, M., Abe, K., Dansako, H., Nakamura, T., Naka, K. & Kato, N. (2005). Efficient replication of a full-length hepatitis C virus genome, strain O, in cell culture, and development of a luciferase reporter system. *Biochem Biophys Res Commun* **329**, 1350–1359.

Ishido, S. & Hotta, H. (1998). Complex formation of the non-structural protein 3 of hepatitis C virus with the p53 tumor suppressor. *FEBS Lett* **438**, 258–262.

Ishido, S., Muramatsu, S., Fujita, T., Iwanaga, Y., Tong, W.-Y., Katayama, Y., Itoh, M. & Hotta, H. (1997). Wild-type, but not mutant-type, p53 enhances nuclear accumulation of the NS3 protein of hepatitis C virus. *Biochem Biophys Res Commun* **230**, 431–436.

Kadoya, H., Nagano-Fujii, M., Deng, L., Nakazono, N. & Hotta, H. (2005). Nonstructural proteins 4A and 4B of hepatitis C virus transactivate the interleukin 8 promoter. *Microbiol Immunol* **49**, 265–273.

Kao, C.-F., Chen, S.-Y., Chen, J.-Y. & Wu Lee, Y.-H. (2004). Modulation of p53 transcription regulatory activity and post-translational modification by hepatitis C virus core protein. *Oncogene* **23**, 2472–2483.

Kim, D. W., Gwack, Y., Han, J. H. & Choe, J. (1995). C-terminal domain of the hepatitis C virus NS3 protein contains an RNA helicase activity. *Biochem Biophys Res Commun* **215**, 160–166.

Kim, J.-E., Song, W. K., Chung, K. M., Back, S. H. & Jang, S. K. (1999). Subcellular localization of hepatitis C viral proteins in mammalian cells. *Arch Virol* **144**, 329–343.

Kwun, H. J., Jung, E. Y., Ahn, J. Y., Lee, M. N. & Jang, K. L. (2001). p53-dependent transcriptional repression of $p21^{waf1}$ by hepatitis C virus NS3. *J Gen Virol* **82**, 2235–2241.

Lan, K.-H., Sheu, M.-L., Hwang, S.-J. & 8 other authors (2002). HCV NS5A interacts with p53 and inhibits p53-mediated apoptosis. *Oncogene* **21**, 4801–4811.

Levine, A. J. (1997). p53, the cellular gatekeeper for growth and division. *Cell* **88**, 323–331.

Lin, C., Prágai, B. M., Grakoui, A., Xu, J. & Rice, C. M. (1994). Hepatitis C virus NS3 serine proteinase: *trans*-cleavage requirements and processing kinetics. *J Virol* **68**, 8147–8157.

Loguercio, C., Cuomo, A., Tuccillo, C., Gazzerro, P., Cioffi, M., Molinari, A. M. & Del Vecchio Blanco, C. (2003). Liver p53 expression in patients with HCV-related chronic hepatitis. *J Viral Hepat* **10**, 266–270.

Lohmann, V., Körner, F., Dobierzewska, A. & Bartenschlager, R. (2001). Mutations in hepatitis C virus RNAs conferring cell culture adaptation. *J Virol* **75**, 1437–1449.

Longworth, M. S. & Laimins, L. A. (2004). Pathogenesis of human papillomaviruses in differentiating epithelia. *Microbiol Mol Biol Rev* **68**, 362–372.

Martin, M. E. D. & Berk, A. J. (1998). Adenovirus E1B 55K represses p53 activation in vitro. *J Virol* **72**, 3146–3154.

McLure, K. G. & Lee, P. W. K. (1998). How p53 binds DNA as a tetramer. *EMBO J* **17**, 3342–3350.

Moss, B., Elroy-Stein, O., Mizukami, T., Alexander, W. A. & Fuerst, T. R. (1990). New mammalian expression vectors. *Nature* **348**, 91–92.

Mottola, G., Cardinali, G., Ceccacci, A., Trozzi, C., Bartholomew, L., Torrisi, M. R., Pedrazzini, E., Bonatti, S. & Migliaccio, G. (2002). Hepatitis C virus nonstructural proteins are localized in a modified endoplasmic reticulum of cells expressing viral subgenomic replicons. *Virology* **293**, 31–43.

Müller-Tiemann, B. F., Halazonetis, T. D. & Elting, J. J. (1998). Identification of an additional negative regulatory region for p53 sequence-specific DNA binding. *Proc Natl Acad Sci U S A* **95**, 6079–6084.

Münger, K. & Howley, P. M. (2002). Human papillomavirus immortalization and transformation functions. *Virus Res* **89**, 213–228.

Muramatsu, S., Ishido, S., Fujita, T., Itoh, M. & Hotta, H. (1997). Nuclear localization of the NS3 protein of hepatitis C virus and factors affecting the localization. *J Virol* **71**, 4954–4961.

Ogata, S., Ku, Y., Yoon, S., Makino, S., Nagano-Fujii, M. & Hotta, H. (2002). Correlation between secondary structure of an amino-terminal portion of the nonstructural proteins 3 (NS3) of hepatitis C virus and development of hepatocellular carcinoma. *Microbiol Immunol* **46**, 549–554.

Ogata, S., Florese, R. H., Nagano-Fujii, M. & 7 other authors (2003). Identification of hepatitis C virus (HCV) subtype 1b strains that are highly, or only weakly, associated with hepatocellular carcinoma on the basis of the secondary structure of an amino-terminal portion of the HCV NS3 protein. *J Clin Microbiol* **41**, 2835–2841.

Qadri, I., Iwahashi, M. & Simon, F. (2002). Hepatitis C virus NS5A protein binds TBP and p53, inhibiting their DNA binding and p53 interactions with TBP and ERCC3. *Biochim Biophys Acta* **1592**, 193–204.

Reed, K. E. & Rice, C. M. (2000). Overview of hepatitis C virus genome structure, polyprotein processing, and protein properties. *Curr Top Microbiol Immunol* **242**, 55–84.

Saito, I., Miyamura, T., Ohbayashi, A. & 10 other authors (1990). Hepatitis C virus infection is associated with the development of hepatocellular carcinoma. *Proc Natl Acad Sci U S A* **87**, 6547–6549.

Sakamuro, D., Furukawa, T. & Takegami, T. (1995). Hepatitis C virus nonstructural protein NS3 transforms NIH3T3 cells. *J Virol* **69**, 3893–3896.

Sheppard, H. M., Corneillie, S. I., Espiritu, C., Gatti, A. & Liu, X. (1999). New insights into the mechanism of inhibition of p53 by simian virus 40 large T antigen. *Mol Cell Biol* **19**, 2746–2753.

Taguchi, T., Nagano-Fujii, M., Akutsu, M., Kadoya, H., Ohgimoto, S., Ishido, S. & Hotta, H. (2004). Hepatitis C virus NS5A protein interacts with 2′,5′-oligoadenylate synthetase and inhibits antiviral activity of IFN in an IFN sensitivity-determining region-independent manner. *J Gen Virol* **85**, 959–969.

Tanaka, M., Nagano-Fujii, M., Deng, L., Ishido, S., Sada, K. & Hotta, H. (2006). Single-point mutations of hepatitis C virus NS3 that impair p53 interaction and anti-apoptotic activity of NS3. *Biochem Biophys Res Commun* **340**, 792–799.

Truant, R., Antunovic, J., Greenblatt, J., Prives, C. & Cromlish, J. A. (1995). Direct interaction of the hepatitis B virus HBx protein with p53 leads to inhibition by HBx of p53 response element directed-transactivation. *J Virol* **69**, 1851–1859.

Waterman, M. J. F., Stavridi, E. S., Waterman, J. L. F. & Halazonetis, T. D. (1998). ATM-dependent activation of p53 involves dephosphorylation and association with 14-3-3 proteins. *Nat Genet* **19**, 175–178.

Weinberg, R. L., Veprintsev, D. B. & Fersht, A. R. (2004). Cooperative binding of tetrameric p53 to DNA. *J Mol Biol* **341**, 1145–1159.

Zemel, R., Gerechet, S., Greif, H. & 7 other authors (2001). Cell transformation induced by hepatitis C virus NS3 serine protease. *J Viral Hepat* **8**, 96–102.

Journal of General Virology (2005), 86, 2197–2208 DOI 10.1099/vir.0.80862-0

Hepatitis C virus NS3 protein interacts with ELKS-δ and ELKS-α, members of a novel protein family involved in intracellular transport and secretory pathways

Rachmat Hidajat,[1] Motoko Nagano-Fujii,[1] Lin Deng,[1] Motofumi Tanaka,[1,2] Yuki Takigawa,[1] Sohei Kitazawa[3] and Hak Hotta[1]

Correspondence
Hak Hotta
hotta@kobe-u.ac.jp

Divisions of Microbiology[1], Gastroenterological Surgery[2] and Molecular Pathology[3], Kobe University Graduate School of Medicine, 7-5-1 Kusunoki-cho, Chuo-ku, Kobe 650-0017, Japan

The NS3 protein of hepatitis C virus (HCV) has a serine protease activity in its N-terminal region, which plays a crucial role in virus replication. This region has also been reported to interact not only with its viral cofactor NS4A, but also with a number of host-cell proteins, which suggests a multifunctional feature of NS3. By means of yeast two-hybrid screening using an N-terminal region of NS3 as bait, a human cDNA encoding a region of ELKS-δ, a member of a novel family of proteins involved in intracellular transport and secretory pathways, was molecularly cloned. Using co-immunoprecipitation, GST pull-down and confocal and immunoelectron microscopic analyses, it was shown that full-length NS3 interacted physically with full-length ELKS-δ and its splice variant, ELKS-α, both in the absence and presence of NS4A, in cultured human cells, including Huh-7 cells harbouring an HCV subgenomic RNA replicon. The degree of binding to ELKS-δ varied with different sequences of the N-terminal 180 residues of NS3. Interestingly, NS3, either full-length or N-terminal fragments, enhanced secretion of secreted alkaline phosphatase (SEAP) from the cells, and the increase in SEAP secretion correlated well with the degree of binding between NS3 and ELKS-δ. Taken together, these results suggest the possibility that NS3 plays a role in modulating host-cell functions such as intracellular transport and secretion through its binding to ELKS-δ and ELKS-α, which may facilitate the virus life cycle and/or mediate the pathogenesis of HCV.

Received 27 December 2004
Accepted 11 April 2005

INTRODUCTION

Hepatitis C virus (HCV) is the causative agent of non-A, non-B hepatitis (Choo *et al.*, 1989). It has been estimated that more than 170 million individuals are infected with HCV worldwide, representing nearly 3% of the world's population (WHO, 1999). The majority of patients remain chronically infected, suffering from chronic liver disorders such as chronic hepatitis, liver cirrhosis and hepatocellular carcinoma (HCC).

HCV, an enveloped RNA virus, belongs to the genus *Hepacivirus* of the family *Flaviviridae*. The HCV genome is a single-stranded, positive-sense RNA of approximately 9·6 kb, which contains a large open reading frame (ORF) flanked by 5′- and 3′-untranslated regions (Reed & Rice, 2000). The ORF encodes a polyprotein of approximately 3000 aa, which is cleaved by the cellular signal peptidase and two virally encoded proteases into at least 10 mature proteins: core, envelope glycoprotein 1 (E1), E2, p7, non-structural protein 2 (NS2), NS3, NS4A, NS4B, NS5A and NS5B (Hijikata *et al.*, 1991, 1993).

NS3 is comprised of two domains, one possessing a serine protease activity and the other an RNA helicase activity, both of which are essential for virus replication. The protease domain resides in the N-terminal part of NS3, while the helicase domain is in the C-terminal part. NS3 enzymic activities are modulated by NS4A, which forms a complex with NS3 to stabilize and localize it to the perinuclear endoplasmic reticulum (ER) membranes (Reed & Rice, 2000; Wölk *et al.*, 2000). NS3 also interacts with the other NS proteins, either directly or indirectly through host-cell proteins, to form the virus replication complex (Aizaki *et al.*, 2004).

The interactions between NS3 and cellular proteins have been studied to elucidate its role(s) in viral pathogenesis (Reed & Rice, 2000; Tellinghuisen & Rice, 2002). The helicase domain of NS3 was shown to interact with protein kinase A (Aoubala *et al.*, 2001; Borowski *et al.*, 1999a). It was

The primer sequences used in this study are available as supplementary material in JGV Online.

also reported that NS3 served as a substrate for protein kinase C (PKC) and inhibited PKC signalling via competition with its physiological substrates (Borowski *et al.*, 1999b). NS3 also binds to histones H2B and H4 (Borowski *et al.*, 1999c). The NS3 helicase domain has also been shown to be essential for NS3 protein methylation by the protein arginine methyltransferase 1 (Rho *et al.*, 2001).

Studies on the NS3 serine protease domain have demonstrated that it can transform NIH3T3 cells (Sakamuro *et al.*, 1995), rat fibroblasts (Zemel *et al.*, 2001) and the human liver cell line QSG7701 (He *et al.*, 2003), although the underlying mechanism(s) remains to be elucidated. Previously, we reported that the oncogenic properties of NS3 might involve an interaction with the tumour suppressor p53 (Ishido & Hotta, 1998; Muramatsu *et al.*, 1997). The protease domain of NS3 has also been reported to bind to Sm-D1, a component of small nuclear ribonucleoprotein associated with autoimmune disease (Iwai *et al.*, 2003). A more recent study demonstrated that the protease domain of NS3 interacts with LMP7, a component of the immunoproteasome, and downregulated the proteasome peptidase activity (Khu *et al.*, 2004).

To identify another possible cellular target(s) that interacts with the NS3 protease domain, we screened a human cDNA library using a yeast two-hybrid system. We have shown here that NS3, through its protease domain, binds to ELKS-δ and its splice variant, ELKS-α (Nakata *et al.*, 1999, 2002). Since a mouse homologue of ELKS-δ, namely Rab6-interacting protein 2B (Rab6IP2B), was reported to affect intracellular transport by binding to Rab6 (Monier *et al.*, 2002), we tested the possible effects of NS3–ELKS-δ interaction on intracellular transport and secretory pathways using a secreted alkaline phosphatase (SEAP) assay. We observed that NS3 augmented the cellular secretion of SEAP and that the increase in SEAP secretion was proportional to the degree of binding between NS3 and ELKS-δ. These results collectively suggest the possibility that NS3 affects intracellular transport and/or secretion pathways by interacting with ELKS-δ and ELKS-α.

METHODS

Plasmid construction. cDNA fragments encoding an N-terminal portion of NS3 (aa 1027–1208) were amplified from sera of HCV-1b-infected patients by RT-PCR as described previously (Ogata *et al.*, 2002, 2003), with minor modifications, using the primers NS3-F and NS3-181R (see Supplementary Table in JGV Online). The amplified fragments were subcloned in frame to the LexA DNA-binding domain of pHybLex/Zeo (Invitrogen) to generate pLex-NS3-H-31 and pLex-NS3-H-45 for expression in yeast. Frame-shift mutants of bait (pLex-NS3-H-31-FS) and prey [pB42-ELKS-δ(787–1063)-FS] were generated by digesting the parental plasmids with *Eco*RI and *Bam*HI, respectively, followed by blunt-end formation and self-ligation. They served as negative controls. pB42-ATF6-α (Tong *et al.*, 2002) was also used as a negative control in this study.

A mammalian expression plasmid encoding Myc-tagged full-length NS3 [pcDNA3.1/NS3F(MKC1a)] was constructed by amplifying a cDNA fragment from pBSNS3/1027–1657 (Muramatsu *et al.*, 1997) using primers NS3/M/B and NS3F*Hin*dIII (Supplementary Table), followed by subcloning into pcDNA3.1/*myc*-His(−)C (Invitrogen). Expression plasmids for chimeric forms of full-length NS3 were constructed, in which the N-terminal 180 residues were derived from clinical isolates, nos 42, 45, H05-5 and H17-2 (Ogata *et al.*, 2002, 2003; GenBank accession nos AB072084, AB072086, AB072048 and AB072055, respectively), while the C-terminal 451 residues were derived from MKC1a (GenBank accession no. D45172). These plasmids were designated pcDNA3.1/NS3(M-42), pcDNA3.1/NS3-(M-45) pcDNA3.1/NS3(M-H05-5) and pcDNA3.1/NS3(M-H17-2), respectively.

A GST fusion protein-expressing plasmid was also constructed. A vector plasmid, pcDNA3.1/GST, was constructed by introducing a 767 bp *Hin*cII fragment of pGEX-4T1 (Pharmacia) into *Eco*RI-digested, blunt-ended pcDNA3.1/*myc*-His(−)C. The full-length NS3-coding region of MKC1a was subcloned in frame to pcDNA3.1/GST to generate pcDNA3.1/GST-NS3. pBS-GST-NS4B-F (Tong *et al.*, 2002) and pBS-GST-NS5A-F (Taguchi *et al.*, 2004) served as negative controls in this study.

Expression plasmids for FLAG-tagged, full-length ELKS-δ and ELKS-α were constructed. cDNA fragments of 3889 and 3834 bp encoding N-terminally deleted ELKS-δ and ELKS-α, respectively, were obtained by digesting pDR2-ELKS-δ and pDR2-ELKS-α (kind gifts from Dr M. Emi, Institute of Gerontology, Nippon Medical School, Kawasaki, Kanagawa, Japan) with *Bam*HI and *Xba*I and subcloned into the pcDNA3.1/N-FLAG vector (Tong *et al.*, 2002). Subsequently, a 718 bp sequence of ELKS-δ or ELKS-α (from the ATG initiation codon to the *Bam*HI site) was amplified by PCR from pDR2-ELKS-δ or pDR2-ELKS-α using the primers ELKS-F and ELKS-303R (Supplementary Table) and subcloned into the above plasmids. The resultant plasmids were designated pcDNA3.1/N-FLAG-ELKS-δ and pcDNA3.1/N-FLAG-ELKS-α. In addition, various deletion mutants of ELKS-δ were constructed by PCR using appropriate sets of primers (Supplementary Table), followed by subcloning into the expression vector.

Yeast two-hybrid screening. Yeast two-hybrid screening was performed using a Hybrid Hunter kit (Invitrogen) and a human cDNA library, as reported previously with some modifications (Tong *et al.*, 2002). In brief, the L40 yeast strain carrying pLex-NS3-H31 was transformed with the pYESTrp cDNA library prepared from HeLa cells (Invitrogen). Transformants were screened for growth on YC-WHUKZ300 plates lacking tryptophan, histidine, uracil and lysine but containing Zeocin. The resultant colonies were tested for β-galactosidase (β-Gal) activity according to the manufacturer's protocol.

Cell culture and protein expression. Vaccinia virus T7 hybrid expression was performed as reported previously (Muramatsu *et al.*, 1997). In brief, HeLa cells were inoculated with recombinant vaccinia virus expressing T7 RNA polymerase (vTF7-3). After virus adsorption for 1 h, cells were transfected with expression plasmids using Lipofectin (Invitrogen) and incubated overnight. Cells were then analysed for possible protein–protein interactions (see below). For immunofluorescence and the SEAP secretion assay, a plasmid-based expression method was employed using Fugene 6 transfection reagent (Roche). Cells were then incubated for 48 h before analysis.

A Huh-7 cell line stably harbouring an HCV subgenomic RNA replicon was prepared as described previously (Lohmann *et al.*, 2001; Taguchi *et al.*, 2004; Takigawa *et al.*, 2004), using pFK2884Gly (a kind gift from Dr R. Bartenschlager, University of Heidelberg, Heidelberg, Germany). A cured Huh-7 cell line was prepared by maintaining the stable HCV replicon-harbouring cell line in the presence of α-interferon (1000 IU ml^{-1}) for 1 month.

Double-staining immunofluorescence. Cells expressing Myc-tagged NS3 and FLAG-tagged ELKS-δ were fixed with 4% paraformaldehyde at room temperature for 15 min and permeabilized with 100% methanol at −20 °C for 3 min. Cells were then blocked with 5% normal donkey serum for 1 h at room temperature. Primary antibodies used were anti-Myc mouse monoclonal antibody (Santa Cruz Biotech) and anti-FLAG rabbit polyclonal antibody (Sigma). FITC-conjugated goat anti-mouse IgG (MBL) and Cy3-conjugated donkey anti-rabbit IgG (Chemicon) were used as secondary antibodies, respectively. Stained cells were observed with a laser-scanning confocal microscope (LSM510 version 3.0; Carl Zeiss) or a fluorescence microscope (BX51; Olympus) attached to a DP70 CCD camera.

Immunoelectron microscopy. Cells expressing Myc-tagged NS3 and FLAG-tagged ELKS-δ were fixed with 4% paraformaldehyde and 0·2% glutaraldehyde for 30 min at room temperature. After washing with PBS, cells were centrifuged at 1500 r.p.m. for 5 min. The cell pellet was dehydrated in a series of 70, 80 and 90% ethanol, embedded in LR White resin (London Resin) and kept at −20 °C for 2 days to facilitate resin polymerization. After ultrathin sectioning, samples were etched in 3% H_2O_2 for 5 min at room temperature and washed with PBS. For labelling, sections were incubated with anti-Myc mouse monoclonal antibody and anti-FLAG rabbit antiserum for 1 h. After rinsing with PBS, sections were incubated with goat anti-mouse IgG and goat anti-rabbit IgG conjugated to 5 and 10 nm gold particles (Sigma), respectively, for 1 h. Sections were post-stained with uranyl acetate and lead citrate and observed under a transmission electron microscope (JEM 1200EX; JEOL).

Co-immunoprecipitation. Cells expressing Myc-tagged NS3 and FLAG-tagged ELKS-δ or ELKS-α were lysed in ice-cold RIPA buffer (1× PBS, 1% NP-40, 0·5% sodium deoxycholate, 0·1% SDS) with freshly added protease inhibitors (PMSF and aprotinin). Lysates were centrifuged at 10 000 *g* for 10 min at 4 °C and the supernatants were mixed with 0·25 μg normal rabbit IgG and 20 μl protein G–agarose beads (Pharmacia) at 4 °C for 30 min to eliminate non-specific binding. The pre-cleared lysates were incubated with anti-Myc rabbit polyclonal antibody for 1 h at 4 °C, followed by incubation with 20 μl protein G–agarose beads for another 1 h. After five washes with ice-cold RIPA buffer, the immunoprecipitates were analysed by immunoblotting, as described below.

Immunoblotting. Samples were subjected to SDS-PAGE and blotted electrophoretically on to a PVDF membrane (Immobilon-P; Millipore). After blocking in PBS containing 5% skimmed milk, membranes were incubated with anti-FLAG or anti-Myc mouse monoclonal antibody for 1 h. Membranes were then incubated with peroxidase-labelled goat anti-mouse IgG (MBL) for 1 h. After three washes, protein bands were visualized by enhanced chemiluminescence (Amersham Biosciences). Densitometric analysis was performed using publicly available software (tnimage-3.3.14; available at http://brneurosci.org/tnimage.html).

GST pull-down assay. Lysates were prepared from cells transiently expressing GST-tagged NS3 and FLAG-tagged ELKS-δ or ELKS-α. Lysates were mixed with 20 μl glutathione-conjugated Sepharose 4B beads at 4 °C for 90 min. The beads were washed five times with ice-cold RIPA buffer and subjected to immunoblot analysis using anti-FLAG antibody. To verify that there was a comparable amount of protein in each sample, lysates were directly (without pull-down) subjected to immunoblotting.

SEAP secretion assay. A SEAP secretion assay was performed to measure the possible effect of NS3 on the secretory pathway. SEAP is a genetically engineered secreted form of alkaline phosphatase (Cullen & Malim, 1992) and the SEAP secretion assay has been widely used to monitor cellular secretory function including Rab6-mediated intracellular transport (Echard *et al.*, 2000; Martinez *et al.*, 1994). HeLa cells were transiently transfected with 200 ng pcDNA3.1-derived NS3 expression plasmid, 50 ng pSEAP2-Control (BD Biosciences) and 1 ng pRL-SV40 (Promega), in the presence or absence of 200 ng pcDNA3.1/N-Flag-ELKS-δ. pRL-SV40 was used to express *Renilla* luciferase as an internal control. After 48 h, culture medium was collected for the SEAP secretion assay, while the cells were processed for the *Renilla* luciferase assay. SEAP activity was measured using the SEAP Reporter Gene Assay (Roche) and *Renilla* luciferase activity measured using the *Renilla* Luciferase Assay System (Promega), according to the manufacturers' instructions. SEAP activity in each sample was normalized against *Renilla* luciferase activity. Since pSEAP2-Control and pRL-SV40 use the same SV40 early promoter, the marginal effect of NS3 on promoter activity (an increase of ~20%, as determined by *Renilla* luciferase activity) was nullified and the effect on SEAP secretion could be determined by this assay.

RESULTS

Identification of ELKS-δ as an NS3-interacting protein using a yeast two-hybrid assay

To identify a human protein(s) that physically interacts with the NS3 protease domain (aa 1027–1208) (Fig. 1a), the L40 yeast strain harbouring pLex-NS3-H-31 was transformed with the pYESTrp-based HeLa cDNA library and screened for growth on YC-WHUKZ300 selection plates. Out of $5{\cdot}8 \times 10^7$ primary transformants screened, 260 colonies grew on the selection plates. Further screening for β-Gal activity identified a clone that showed strong reactivity. DNA sequence analysis revealed that the yeast clone carried a pYESTrp-driven sequence that completely matched the sequence for a C-terminal portion of ELKS-δ (GenBank accession no. AB053470; Nakata *et al.*, 2002). The cloned cDNA fragment was designated ELKS-δ(787–1063).

The specificity of the interaction between NS3 and ELKS-δ(787–1063) was tested by transfecting the parental (naïve) L40 strain with various combinations of expression plasmids, including two different NS3 sequences (H-31 and H-45) and frame-shift mutants of NS3-H-31 and ELKS-δ(787–1063). The results demonstrated specific interaction between the NS3 protease domain and ELKS-δ(787–1063) in yeast (Fig. 1b).

NS3 interacts with ELKS-δ and its splice variant, ELKS-α, in cultured human cells

The interaction between NS3 and ELKS-δ was further investigated in mammalian cells and a specific interaction between the protease domain of NS3 and ELKS-δ(787–1063) was observed (data not shown). Moreover, full-length NS3 (aa 1027–1657) was shown to interact with ELKS-δ(787–1063) in HeLa cells (Fig. 2a, lane 2). We then narrowed down the region of ELKS-δ responsible for the interaction with full-length NS3 (Fig. 2b). C-terminal truncation of ELKS-δ up to aa 1008 did not affect the interaction with NS3. However, further deletion up to aa 995 or 979 abolished the ability to interact with NS3. N-terminal truncation of the initial fragment up to aa 846 did

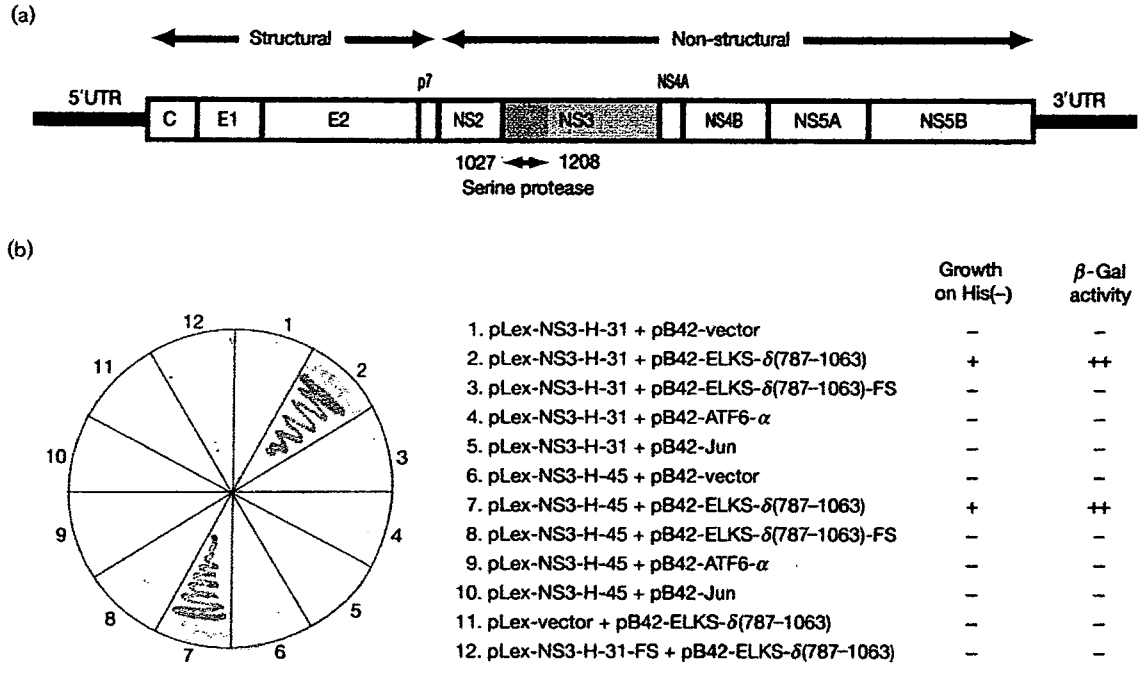

Fig. 1. Identification of ELKS-δ as an NS3-binding protein by yeast two-hybrid assay. (a) Schematic diagram of the HCV genome. The N-terminal serine protease domain of NS3 (aa 1027–1208) used as bait is also depicted. (b) A representative result showing specific interaction between the NS3 protease domain and ELKS-δ(787–1063). The L40 yeast strain co-transfected with the indicated plasmids was grown on tryptophan-deficient media containing the antibiotic Zeocin and subsequently assayed for β-Gal activity. Development of a blue colour within 30 min indicated strong interaction between the two proteins of interest. + +, Strong interaction; +, moderate interaction; –, no interaction.

not affect the interaction with NS3, while further deletion up to aa 876 or 886 completely abolished it. These results mapped a minimum NS3-interacting region somewhere between aa 846 and 1008 of ELKS-δ. ELKS-δ(846–1008) consistently interacted with NS3. Similar results were obtained using a yeast two-hybrid system (data not shown).

Next, we tested the interaction of full-length NS3 with full-length ELKS-δ and its splice variant, ELKS-α. GST pull-down analysis demonstrated that full-length NS3 interacted with full-length ELKS-δ and ELKS-α (Fig. 3a). The specificity of the interaction between NS3 and ELKS-δ was confirmed by demonstrating that neither NS4B nor NS5A of HCV bound to full-length ELKS-δ under the same experimental conditions (Fig. 3b). Specific interaction between the two molecules was also confirmed by co-immunoprecipitation analysis, in which anti-FLAG antibody (directed against FLAG-tagged full-length ELKS-δ and ELKS-α) co-immunoprecipitated full-length NS3 (data not shown).

In order to determine whether NS3 interacted with ELKS proteins in the presence of the other HCV non-structural proteins, we expressed ELKS-δ and ELKS-α in Huh-7 cells harbouring an HCV subgenomic RNA replicon and subsequently immunoprecipitated NS3 using anti-NS3 polyclonal antibody. The result demonstrated that NS3 expressed in the context of HCV replication interacted with full-length ELKS-δ and ELKS-α in HCV RNA replicon-harbouring cells (Fig. 3c).

Sequence comparison of ELKS-δ and ELKS-α

The amino acid sequences of ELKS-δ and ELKS-α differ from each other in their C-termini due to alternative splicing (Fig. 4a). As described above, a minimum region responsible for the interaction with NS3 was mapped between aa 846 and 1008 of ELKS-δ (Fig. 2). Since full-length ELKS-α interacted with NS3 (Fig. 3), we then determined a minimum region of ELKS-α responsible for the interaction. Deletion mutational analysis revealed that ELKS-α(747–948), but not ELKS-α(763–948), ELKS-α(791–948) or ELKS-α(806–948), interacted with NS3 (Fig. 4b and c), suggesting that ELKS-α(747–948) is the minimum region responsible for the interaction with NS3.

NS3 co-localizes with ELKS-δ in human cells

We visualized the co-localization of NS3 with ELKS-δ in Huh-7 cells by double-staining immunofluorescence

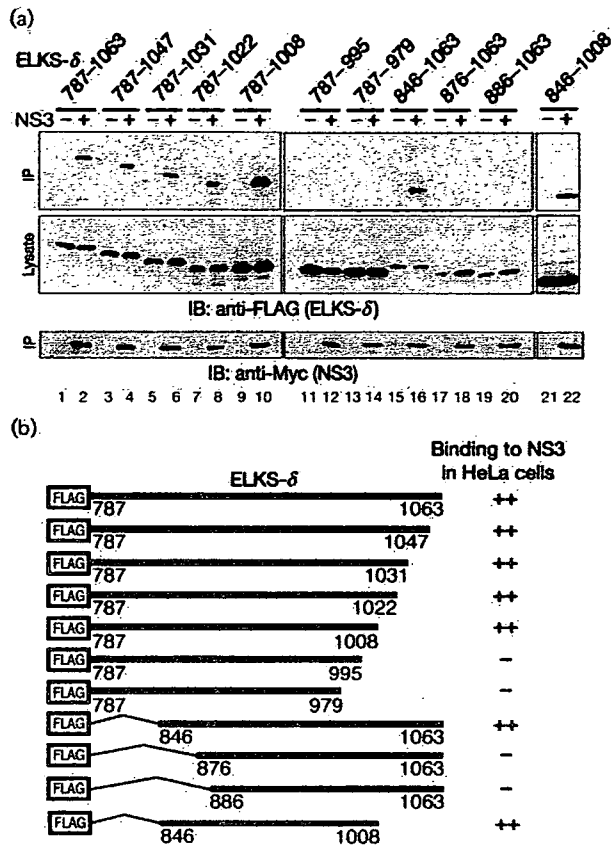

Fig. 2. Determination of the minimum region of ELKS-δ required for interaction with full-length NS3 in cultured human cells. (a) A series of deletion mutants of FLAG-tagged ELKS-δ was expressed by the vaccinia–T7 hybrid expression method in HeLa cells without (odd-numbered lanes) or with (even-numbered lanes) Myc-tagged full-length NS3. Cell lysates were immunoprecipitated using anti-Myc antibody and probed by immunoblotting using anti-FLAG antibody (upper panel). Lysates were directly (without being immunoprecipitated with anti-Myc antibody) probed with anti-FLAG antibody to verify a comparable degree of expression of the ELKS-δ mutants (middle panel). Efficient immunoprecipitation of Myc-tagged NS3 with anti-Myc antibody was also verified (lower panel). (b) Schematic diagram of the various deletion mutants of ELKS-δ. ++, Strong interaction; –, no interaction.

analysis. When co-expressed in Huh-7 cells using plasmid-based expression methods, full-length NS3 co-localized with full-length ELKS-δ in the cytoplasm, both in the absence (Fig. 5a) and presence (Fig. 5b) of NS4A. Co-localization of NS3 with ELKS-δ was also observed in HCV RNA replicon-harbouring cells (Fig. 5c).

Immunoelectron microscopic analysis also demonstrated co-localization of full-length NS3 with full-length ELKS-δ in close proximity to the ER membranes in the perinuclear region (Fig. 5d).

NS3 interacts differentially with ELKS-δ in an NS3 sequence-dependent manner

A considerable degree of sequence variation has been observed in the N-terminal 180 residues of NS3 (Ogata *et al.*, 2002, 2003). We performed experiments to determine whether or not interaction with ELKS-δ varied with different NS3 sequences. We first used 198-residue fragments of NS3 obtained from four patients (nos 42, 45, H05-5 and H17-2) and found that the degree of interaction with ELKS-δ varied with the different sequences (data not shown). Next, we tested full-length NS3 sequences of five different isolates, a parental strain (MKC1a) and four chimeric forms (M-42, M-45, M-H05-5 and M-H17-2), which differed from each other by at most 10 residues within the N-terminal 180 residues, all having the remaining C-terminal 451 residues in common. These full-length forms of NS3 were each expressed with full-length ELKS-δ and the interactions examined. Consistent with the results obtained with the 198-residue fragments, the degree of interaction between full-length NS3 and ELKS-δ varied with the different NS3 sequences, with M-42 and M-45 showing the strongest interaction, and M-H05-5 the weakest (Fig. 6a and b). Sequence alignment of the N-terminal 180 residues of NS3 is shown in Fig. 6(c). Five residues (Val-1044, Leu-1106, Ala-1176, Val-1179 and Ile-1196) were unique to M-H05-5. Based on this sequence alignment alone, however, it was difficult to draw a conclusion as to which residue(s) most significantly affects the interaction with ELKS-δ.

When NS4A was co-expressed, the interaction between NS3 and ELKS-δ became weaker, although still detectable, and the NS3 sequence-dependent difference in the interaction with ELKS-δ was not clearly observed (data not shown).

NS3 enhances SEAP secretion from the cell, possibly through its interaction with ELKS-δ

The binding domain of Rab6IP2, a murine homologue of ELKS-δ, has been reported to affect the endosome-to-Golgi retrograde transport pathway through its binding to Rab6 (Monier *et al.*, 2002). CAST and ERC proteins, rat homologues of the ELKS protein family, have also been implicated in the modulation of neurotransmitter secretion (Deguchi-Tawarada *et al.*, 2004; Ohtsuka *et al.*, 2002; Wang *et al.*, 2002). We thought that NS3 might affect the possible function of ELKS-δ and/or its splice variant(s), modulating intracellular transport and secretory function. Therefore, we performed a SEAP assay. The results demonstrated that SEAP secretion was significantly enhanced by NS3 of three isolates (MKC1a, M-42 and M-45), especially when ELKS-δ was expressed ectopically (Fig. 7a). In this context, we assumed that endogenous ELKS-δ was also expressed, although to a lesser extent. In contrast, NS3 of the other isolates (M-H-05-5 and M-H17-2) did not enhance SEAP secretion in the absence of ectopic ELKS-δ, while a mild enhancement by NS3 of M-H17-2 was

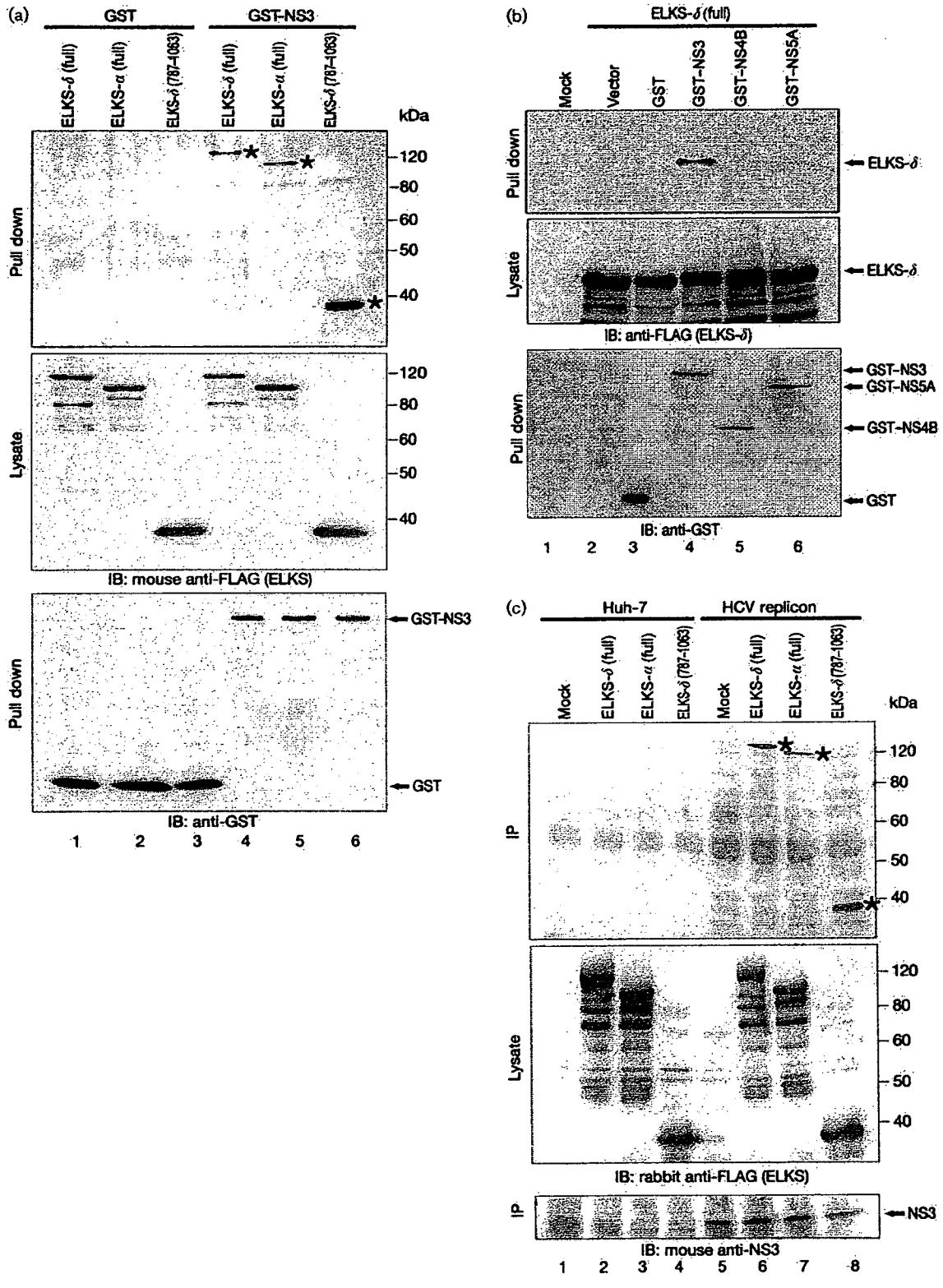

observed when ELKS-δ was expressed ectopically. Interestingly, the degree of interaction between NS3 and ELKS-δ correlated well with the level of increase in SEAP secretion (Fig. 7b). Moreover, SEAP secretion was enhanced in HCV RNA replicon-harbouring Huh-7 cells compared with HCV RNA-negative Huh-7 cells that had been cured by interferon treatment (Fig. 7c). These results strongly suggested that NS3 affects the cellular secretory pathway by interacting with ELKS-δ and ELKS-α.

Fig. 3. Full-length ELKS-δ and ELKS-α interact with full-length NS3 in cultured human cells. (a) FLAG-tagged full-length ELKS-δ (lanes 1 and 4), full-length ELKS-α (lanes 2 and 5) and a deletion mutant, ELKS-δ(787–1063) (lanes 3 and 6), were co-expressed in HeLa cells with GST (lanes 1–3) or full-length NS3 fused to GST (lanes 4–6). Cell lysates were pulled down with glutathione beads and probed with anti-FLAG antibody (upper panel). Lysates were directly (without being pulled down) probed with anti-FLAG antibody to confirm expression of ELKS-δ or ELKS-α (middle panel). Efficient pull-down was also verified (lower panel). (b) FLAG-tagged full-length ELKS-δ was co-expressed in HeLa cells with empty vector (lane 2), GST (lane 3), GST-tagged full-length NS3 (lane 4), full-length NS4B (lane 5) and full-length NS5A (lane 6). Cells lysates were pulled down by glutathione beads and probed with anti-FLAG antibody (upper panel). Lysates were directly probed with anti-FLAG antibody to confirm ELKS-δ expression (middle panel). Efficient pull down was also verified (lower panel). (c) FLAG-tagged full-length ELKS-δ (lanes 2 and 6), full-length ELKS-α (lanes 3 and 7) and a deletion mutant, ELKS-δ(787–1063) (lanes 4 and 8), were expressed in Huh-7 cells harbouring an HCV RNA replicon (lanes 5–8) or parental Huh-7 cells as a control (lanes 1–4). Cell lysates were immunoprecipitated with anti-NS3 polyclonal antibody and probed with anti-FLAG antibody (upper panel). Expression of ELKS-δ and ELKS-α (middle panel) and efficient immunoprecipitation of NS3 (lower panel) were also verified.

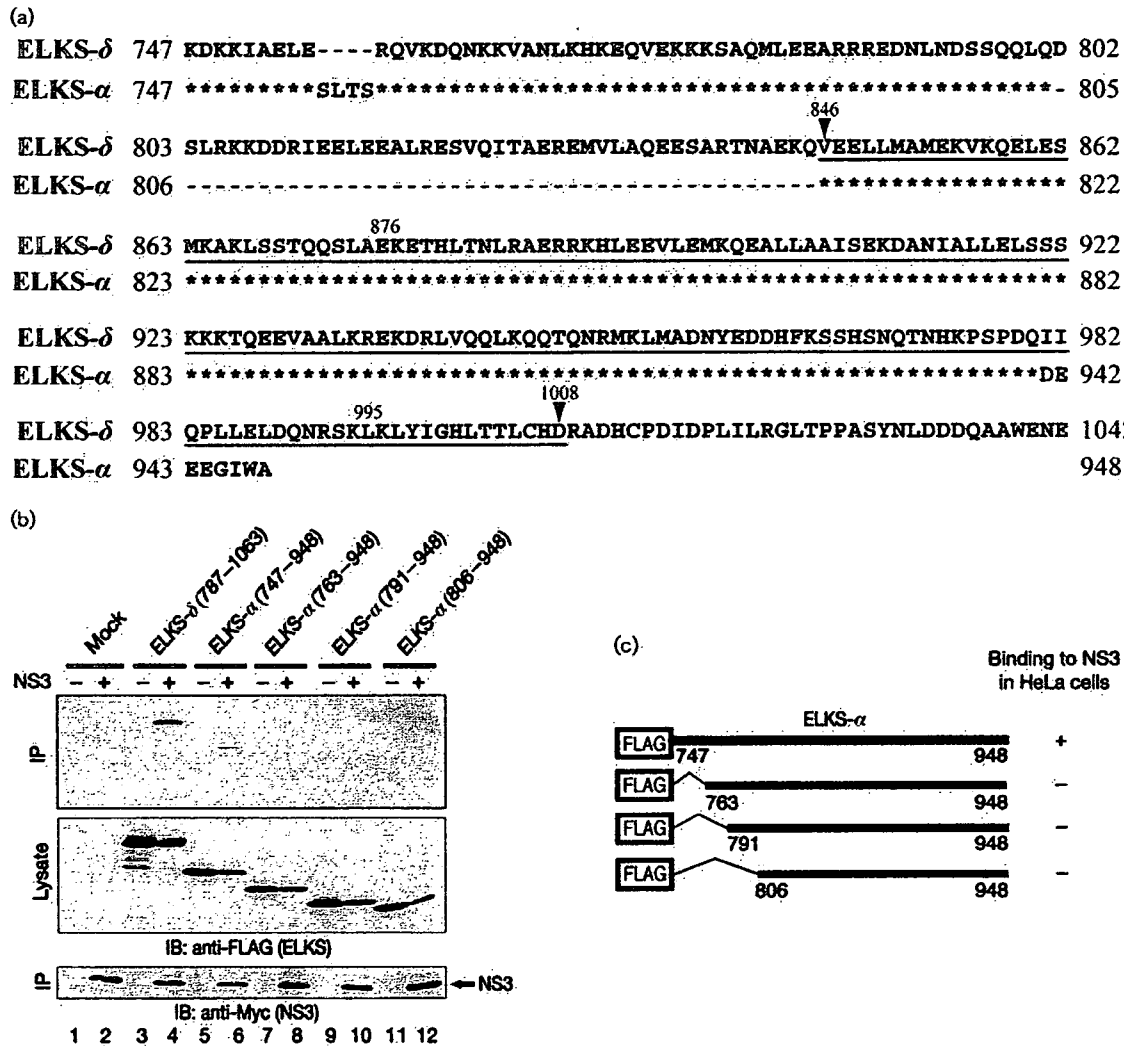

Fig. 4. Sequence comparison of C-terminal portions of ELKS-δ and ELKS-α. (a) Sequence alignment of a C-terminal portion of ELKS-δ and ELKS-α. Asterisks indicate identical residues. Hyphens indicate missing residues when compared with the other isoform. Underlined (aa 846–1008) is the minimum region of ELKS-δ required for interaction with NS3 (see Fig. 2). (b) A series of deletion mutants of FLAG-tagged ELKS-α was expressed without (odd-numbered lanes) or with (even-numbered lanes) Myc-tagged full-length NS3. ELKS-δ(787–1063) (lanes 3 and 4) served as a positive control. Cell lysates were immunoprecipitated using anti-Myc antibody and probed with anti-FLAG antibody (upper panel). Lysates were directly probed with anti-FLAG antibody to confirm expression of the ELKS-α mutants (middle panel). Efficient immunoprecipitation of NS3 was also verified (lower panel). (c) Schematic diagram of the ELKS-α deletion mutants. +, Moderate interaction [weaker than ELKS-δ(787–1063)]; –, no interaction.